

President's Address

It is a pleasure to inform all EUROMECH members of the outcome of the recent EUROMECH Council elections, as reported in detail elsewhere in this issue of the Newsletter. Let me here very simply welcome to the Council the following distinguished colleagues: Professor Jensen (University of Nottingham, Fluids), Professor Petryk (Institute of Fundamental Technological Research, Warsaw, Solids) and Doctor Raous (Laboratory of Mechanics and Acoustics, Marseille, Solids). They will serve on the Council for six years from 1 January 2007. We will benefit greatly from their involvement in all aspects of EUROMECH activities and we wish them all a highly successful term of office. Thank you also to EUROMECH members for having renewed their confidence in me. It is an honour and a responsibility.

I would like to thank the other candidates who stood for election and did not on this occasion get elected. There was strong support for all of them and I very much hope that they will remain actively involved in EUROMECH activities.

On behalf of the Council, let me also express our gratitude to the three colleagues who ended their term on the council at the end of 2006: Professor David Abrahams (University of Manchester, Fluids), Professor Ahmed Benallal (Laboratory of Mechanics and Technology, Cachan, Solids) and Professor Irina Goryacheva (Institute for Problems in Mechanics, Moscow, Solids). It was very pleasant to work with them in the last six years and their contributions to the well-being of EUROMECH were very much appreciated.

Be sure to remain informed of all EUROMECH events through our website www.euromech.org, which is expertly managed by Doctor Sara Guttilla in Udine. We are naturally open to your suggestions for making it an even more effective means of communication with all of you.

Patrick Huerre

President, EUROMECH

Contents

President's Address.....	1
EUROMECH Council Members.....	4
Chairpersons of Conference Committees	4
EUROMECH Council Elections	5
EUROMECH Fluid Mechanics Prize Lecture.....	6
<i>"Liquid Sloshing in Cylindrical Containers"</i>	6
EUROMECH Young Scientist Prize Paper	21
<i>"Generation of Prescribed Extensional Waves in an Elastic Bar by Use of Piezoelectric Actuators"</i>	21
EUROMECH Fluid Mechanics Fellow 2006 Paper.....	30
<i>"Transition to Turbulence in Pipe Flow"</i>	30
EUROMECH Fellows: Nomination Procedure.....	38
EUROMECH Prizes: Nomination Procedure.....	41
EUROMECH Conferences in 2007, 2008, 2009.....	43
EUROMECH Colloquia in 2007 and 2008.....	45
EUROMECH Colloquia Reports	51
EUROMECH Colloquium 475.....	51
<i>"Fluid Dynamics in High Magnetic Fields"</i>	51
EUROMECH Colloquium 479.....	53
<i>"Numerical Simulation of Multiphase Flow with Deformable Interfaces"</i>	53
EUROMECH Colloquium 480.....	54
<i>"High Rayleigh Number Convection"</i>	54
EUROMECH Colloquium 484.....	56
<i>"Wave Mechanics and Stability of Long Flexible Structures Subject to Moving Loads and Flows"</i>	56
EUROMECH Colloquium 487.....	59
<i>"Structure Sensitive Mechanics of Polymer Materials: Physical and Mechanical Aspects"</i>	59
Objectives of EUROMECH, the European Mechanics Society	61

Addresses for EUROMECH Officers

President: Professor Patrick Huerre
Laboratoire d'Hydrodynamique, Ecole Polytechnique
F - 91128 Palaiseau cedex, France
E-mail: huerre@ladhyx.polytechnique.fr
Tel.: +33-(0)1 6933 4990
Fax: +33-(0)1 6933 3030

Vice President: Professor Hans-H. Fernholz
Hermann-Föttinger-Institut, Technische Universität Berlin
Müller-Breslau Strasse 8
D-10623 Berlin, Germany
E-mail: fernholz@hobo.pi.tu-berlin.de
Tel.: +49-(0)30 314 23359
Fax: +49-(0)30 314 21101

Secretary-General: Professor Bernhard Schrefler
Dipartimento di Costruzioni e Trasporti
Università di Padova, Via Marzolo 9
I-35131 Padova, Italy
E-mail: bas@dic.unipd.it
Tel.: +39 049 827 5611
Fax: +39 049 827 5604

Treasurer: Professor Wolfgang Schröder
Chair of Fluid Mechanics and Institute of Aerodynamics
RWTH Aachen, Wüllnerstr. zw. 5 u 7
D-52062 Aachen, Germany
E-mail: office@aia.rwth-aachen.de
Tel.: +49-(0)241 809 5410
Fax: +49-(0)241 809 2257

Newsletter editors:
Dr Roger Kinns: RogerKinns@aol.com
Professor Bernhard Schrefler: bas@dic.unipd.it

Newsletter Assistant:
Dr Sara Guttilla: S.Guttilla@cism.it

Web page: <http://www.euromech.org>

EUROMECH Council Members

PATRICK HUERRE, Laboratoire d'Hydrodynamique, Ecole Polytechnique, 91128 Palaiseau cedex, France — *E-mail: huerre@ladhyx.polytechnique.fr*

HANS H. FERNHOLZ, Herman – Föttinger - Institut für Strömungsmechanik, Technische Universität Berlin, Müller-Breslau Strasse 8, 10623 Berlin, Germany — *E-mail: fernholz@pi.tu-berlin.de*

BERNHARD A. SCHREFLER, Dipartimento di Costruzioni e Trasporti, Università di Padova, Via Marzolo 9, I-35131 Padova, Italy — *E-mail: bas@dic.unipd.it*

WOLFGANG SCHRÖDER, Chair of Fluid Mechanics and Institute of Aerodynamics RWTH Aachen, Wüllnerstr. Zw. 5 u. 7, 52062 Aachen, Germany — *E-mail: o.ce@aia.rwth-aachen.de*

JORGE A.C. AMBRÓSIO, IDMEC, Instituto Superior Técnico, Av. Rovisco Pais 1, 1049-001 Lisboa, Portugal — *E-mail: jorge@dem.ist.utl.pt*

OLIVER E. JENSEN, School of Mathematical Sciences, University of Nottingham, NG72RD, United Kingdom — *E-mail: Oliver.Jensen@nottingham.ac.uk*

DETLEF LOHSE, University of Twente, Department of Applied Physics, P.O. Box 217, 7500 AE Enschede, The Netherlands — *E-mail: d.lohse@utwente.nl*

HENRIK MYHRE JENSEN, Department of Building Technology and Structural Engineering, Aalborg University, Sohngaardsholmsvej 57, DK-9000 Aalborg, Denmark — *E-mail: hmj@civil.auc.dk*

HENRIK PETRYK, Institute of Fundamental Technological Research, Polish Academy of Sciences, Swietokrzyska 21, 00-049 Warsaw, Poland — *E-mail: hpetryk@ippt.gov.pl*

MICHEL RAOUS, Laboratory of Mechanics and Acoustics –CNRS, 31 Chemin Joseph Aiguier, 13402 Marseille Cedex 20, France — *E-mail: raous@lma.cnrs-mrs.fr*

Chairpersons of Conference Committees

GERTJAN F. VAN HEIJST (*Fluid Mechanics*), Eindhoven University of Technology, Physics Dept., Fluid Dynamics Lab., W&S Building, P.O. Box 513, NL-5600 MB Eindhoven, The Netherlands — *E-mail: G.J.F.v.Heijst@fdl.phys.tue.nl*

DOMINIQUE LEGUILLON (*Mechanics of Materials*), Laboratoire de Modélisation en Mécanique, Université Pierre et Marie Curie, Couloir 55-65, case courrier 162, 4 place Jussieu, 75252 Paris Cedex 05, France — *E-mail: leguillo@lmm.jussieu.fr*

DICK H. VAN CAMPEN (*Nonlinear Oscillations*), Eindhoven University of Technology, Mechanical Engineering Department, Den Dolech 2, P.O. Box 513, 5600 MB Eindhoven, The Netherlands — *E-mail: d.h.v.campen@tue.nl*

AHMED BENALLAL (*Solid Mechanics*), LMT, ENS Cachan, 61 Ave. du Président Wilson, 94253 Cachan, France — *E-mail: benallal@lmt.ens-cachan.fr*

ARNE V. JOHANSSON (*Turbulence*), Royal Institute of Technology, Department of Mechanics, 10044 Stockholm, Sweden — *E-mail: viktor@mech.kth.se*

EUROMECH Council Elections

At the end of 2006, four seats on the EUROMECH Council became vacant. After consultation with the advisory board, the affiliated organisations and suggestions made by EUROMECH members, the following members stood for election to the Council for a six-year term starting 1 January 2007.

Slot n°1	P. Huerre (F)	
Slot n°2	N. Morozov (S)	H. Petryk (S)
Slot n°3	O. Jensen (F)	M. G. Worster (F)
Slot n°4	O. Allix (S)	M. Raous (S)

Generally, two candidates stand for one seat and this was the case in slots 2 to 4. This rule is not an obligation imposed by the statutes: when there are good reasons, this unwritten rule needs not to be applied. This was the case in slot 1 because P. Huerre has accepted to continue serving as President in 2007.

The ballot sheet was sent to 1203 regular EUROMECH members. A total of 447 ballots were returned to the Treasurer, which is more than 1/3 of the ballots sent out and required by the statutes for the election to be valid.

The tallying was performed by Wolfgang Schröder, Monika Wiechol and Lidy Willemsen.

The result is as follows:

Slot n°1	P. Huerre (F)	406		
Slot n°2	N. Morozov (S)	166	H. Petryk (S)	219
Slot n°3	O. Jensen (F)	220	M. G. Worster (F)	178
Slot n°4	O. Allix (S)	186	M. Raous (S)	207
Invalid				4

P. Huerre (Ecole Polytechnique), H. Petryk (Institute of Fundamental Technological Research, Warsaw), O. Jensen (University of Nottingham) and M. Raous (Laboratory of Mechanics and Acoustics, Marseille) are therefore elected to the EUROMECH Council. The composition of the new Council is given in this Newsletter.

Aachen, April 2007
W. Schröder, Treasurer

EUROMECH Fluid Mechanics Prize Lecture

“Liquid Sloshing in Cylindrical Containers”

Emil Hopfinger won the EUROMECH Fluid Mechanics Prize, awarded at the sixth EUROMECH Fluid Mechanics Conference held in Stockholm, June 2006

E.J. Hopfinger

LEGI/CNRS, INPG, UJF, B.P. 53, 38041 Grenoble, France

Abstract

In this paper, results are presented on asymmetric sloshing in partially filled circular cylinders subjected to horizontal, periodic forcing, as well as geyser formation and the subsequent axi-symmetric sloshing that is caused by a sudden change in Bond number. Asymmetric sloshing is controlled by three parameters that are the liquid depth parameter, the frequency offset (depending on forcing frequency and forcing amplitude) and the damping. The results cover a wide range of forcing frequencies and forcing amplitudes in the asymptotic limit of large fluid depth and low viscosity liquids. Emphasis is placed on the bounds of existence of the different wave amplitude responses, namely planar waves, swirling waves and breaking waves. In the chaotic regime wave breaking occurs quasi periodically: growth of planar wave amplitude, collapse, irregular swirl and again growth of planar wave amplitude. Geyser formation and axi-symmetric sloshing is initiated by dam-break experiments. This problem is encountered in liquid-propellant fuel tanks where under micro-gravity conditions the liquid rises near the container wall; a sudden increase in axial acceleration can cause geyser formation followed by violent liquid sloshing and gas entrainment.

1. Introduction

Liquid sloshing is frequently encountered in liquid storage tanks subjected to external excitations. The forces exerted on the container walls by the sloshing motions and possible large pressure changes caused by enhanced evaporation or condensation at the liquid-gas interface can lead to accidents. Sloshing is also an interesting fundamental problem, related to non-linear oscillators and dynamic systems (Miles 1984b, Funakoshi and Inoue 1988). The book of Ibrahim (2005) gives a detailed summary of the theory and fundamentals of sloshing under widely different conditions.

During the early developments of space flights, liquid sloshing in fuel tanks received considerable attention. A collection of this research can be found in

Abramson (1966). The sloshing wave modes were analysed in detail for containers of various geometries, including non-linear sloshing and geometric effects on the damping of the liquid motion. The fluid depth is important because resonant waves have negative or positive non-linearity, depending on the liquid depth relative to the tank base dimension (Miles 1984a, Waterhouse 1994, Faltinsen et al. 2003). An interesting aspect is that in circular, cylindrical containers, as well as in square-base cylindrical containers, large amplitude asymmetric waves bifurcate to a swirling wave motion at forcing frequencies near and above the natural frequency, depending on forcing amplitude and fluid depth (Abramson 1966, Miles 1984b, Faltinsen et al 2003).

Most of the time the containers are subjected to low frequency, lateral forcing giving rise to asymmetric gravity wave motions. Vertical forcing, parallel to the container axis, can give rise to symmetric or asymmetric wave modes known as parametric or Faraday instability. Impulsive forcing is also encountered in rocket engine fuel tanks during engine restart. This can lead to geyser formation and subsequent axi-symmetric sloshing. An example of impulsive forcing after a micro-gravity phase is the falling coffee cup experiment by Milgram (1969). Baumbach et al. (2005) used membranes (simulating high surface tension) to obtain small, initial Bond numbers. Rupture of the membrane leads to a sudden increase in Bond number. A rigid barrier can also be used instead of a membrane and some results are shown herein.

In order to scale up results obtained in tanks of laboratory size to large tanks, it is necessary to determine the relevant control or similarity parameters. For a circular, cylindrical tank, subjected to horizontal forcing of tank displacement $x = A_f \sin \omega t$, Miles' weakly nonlinear theory (Miles 1984b) contains three parameters (the Bond number is assumed to be large so that surface tension effects are negligible on the tank scale). These parameters are the frequency offset β , the length scale parameter ℓ / R and the damping parameter α . For the lowest asymmetric wave mode of natural frequency ω_1 these non-dimensional parameters are respectively:

$$\beta = \frac{\omega^2 - \omega_1^2}{\varepsilon^2 \omega_1^2} \quad (1)$$

$$\frac{\ell}{R} = \frac{1}{1.841} \tanh(1.841h/R) \quad (2)$$

$$\alpha = 2\delta / \varepsilon^2 \quad (3)$$

where δ is the damping ratio. For large fluid depth, $h/R > 1.5$, with R the tank radius, damping occurs predominantly in the side wall Stokes boundary layers and is of the form

$$\delta = C_1(\nu^2 / R^3 g)^{1/4} \quad (4)$$

where ν is the kinematic viscosity. For the lowest asymmetric mode $C_1 \approx 1$ (Royon-Lebeaud et al. 2007). The small parameter ε in (1) and (3) is

$$\varepsilon = \left(1.684 \frac{A_f}{R}\right)^{1/3} \quad (5)$$

Theoretically, this parameter must be $\varepsilon \ll 1$, but experiments show (Royon-Lebeaud et al. 2007) that the theory remains valid to leading order when ε is as large as 0.5. The natural frequency of the lowest asymmetric mode is $\omega_1 \equiv \omega_{11} = \left[g k_{11} \left(1 + \frac{k_{11}^2 \sigma}{g \rho}\right) \tanh(k_{11} h) \right]^{1/2}$. When the Bond number is large, the surface tension term in the dispersion relation is negligible and when, in addition $h/R > 1.5$, the dispersion relation reduces to $\omega_1 = \sqrt{g k_1}$, where the wave number $k_1 \equiv k_{11} = 1.841/R$. It is of interest to point out that there is a critical non-dimensional depth $h/R = 0.506$ below which the nonlinearity changes from negative to positive and a depth $h/R = 0.15$, below which harmonics dominate.

First, we present experimental results on large amplitude sloshing and wave breaking in circular, cylindrical containers for large fluid depths, $h/R > 1.5$. In a square-base cylindrical container results are similar. Then we consider dam-break experiments in a circular cylinder that allow simulation of impulsive forcing leading to geyser formation and axis-symmetric sloshing. Section 2 contains a description of the experimental configuration and results of asymmetric sloshing and in Section 3 the results of the dam-break experiments are presented.

2. Lateral Forcing Experiments

2.1 Experimental conditions

The asymmetric sloshing experiments were conducted in circular, cylindrical containers, one of diameter $d = 2R = 300 \pm 4$ mm and 600 mm deep, made of Plexiglas and the other of diameter $d = 156 \pm 0.6$ mm and 250 mm deep, made of Pyrex. The natural periods of the lowest asymmetric modes are respectively $T_1 = 2\pi/\omega_1 = 572$ ms and 413 ms. These containers, filled with water or alcohol to the desired depth h , were mounted on an oscillating table. The fill ratio was always $h/R > 1.2$ (generally 1.5) satisfying deep-water conditions ($\tanh(k_1 h) > 0.976$ in the dispersion relation). Water and alcohol were used. The Bond number on the tank scale is $Bo = \frac{\rho g R^2}{\sigma} > 800$ so that surface tension effects are negligible. Only the sizes of drops and bubble produced by breaking depend on surface tension.

The containers were subjected to a horizontal displacement $x = A_f \sin \omega t$ in the range $0.5 \leq f \leq 5$ Hz and $0.05 \leq A_f \leq 5$ mm. The forcing frequency f ($\omega = 2\pi f$) and forcing amplitude A_f were measured to high accuracy with an optical displacement probe. The wave amplitude was measured with capacitance probes that were calibrated before and after each experiment and have a resolution of 0.2mm. These probes were positioned close to the tank wall and along a line parallel to the tank movement ($\theta = 0^\circ$, position *P1*) and perpendicular ($\theta = 90^\circ$, position *P2*) to the direction of the tank movement. The probe at *P2* indicated whether or not a swirling wave component was present. The shape of the liquid surface was obtained by visualization using backlighting and image analysis.

2.2 Results

2.2.1 Amplitude response curves

Figure 1 shows the wave amplitude response $b = \eta(R, \theta, nT)$, at $\theta = 0^\circ$ (*P1*) and $\theta = 90^\circ$ (*P2*) made dimensionless by the wavelength λ , as a function of dimensionless frequency ω/ω_1 for four forcing amplitudes A_f/R . All experimental points correspond to steady-state wave motions. The open symbols indicate planar waves and the closed symbols swirling waves. The wave amplitude is here scaled by the wavelength of the lowest natural mode, $\lambda \equiv \lambda_1 = 3.411R$. The amplitude response curves show clearly that the limits of existence of steady-state planar waves depend on both, the forcing frequency and forcing amplitude, that are combined in the frequency-offset parameter (1), $\beta = \frac{\omega^2 - \omega_1^2}{\varepsilon^2 \omega_1^2}$. For the four dimensionless forcing amplitudes $A_f/R = 0.0266$, 0.0133, 0.0066 and 0.0033 shown in Figure 2, the parameter ε , given by (5) is respectively $\varepsilon = 0.356$, 0.282, 0.224 and 0.177. The damping parameter (3) is respectively $\alpha \approx 0.061$, 0.098, 0.155 and 0.248 for the four forcing amplitudes and water (for alcohol the α values are about 20% larger). These values of the damping parameters are indicative of small damping where the resonance curves are qualitatively similar, exhibiting at least four bifurcation points when the depth parameter $\frac{\ell}{R} = \frac{1}{1.841} \tanh(1.841h/R)$ is constant, that is when h/R is large.

Above the natural frequency, $\omega/\omega_1 > 1$, when for a given forcing amplitude the forcing frequency is slowly decreased by small decrements, the planar wave amplitude increases (soft spring behavior) until a critical frequency is reached at which the motion bifurcates to a swirling wave; this bifurcation point is denoted as β_d by Miles (1984b). The same bifurcation to a swirling wave mode is obtained when the forcing frequency is fixed and the forcing amplitude is

increased by small increment. The stability boundary is, therefore, well defined.

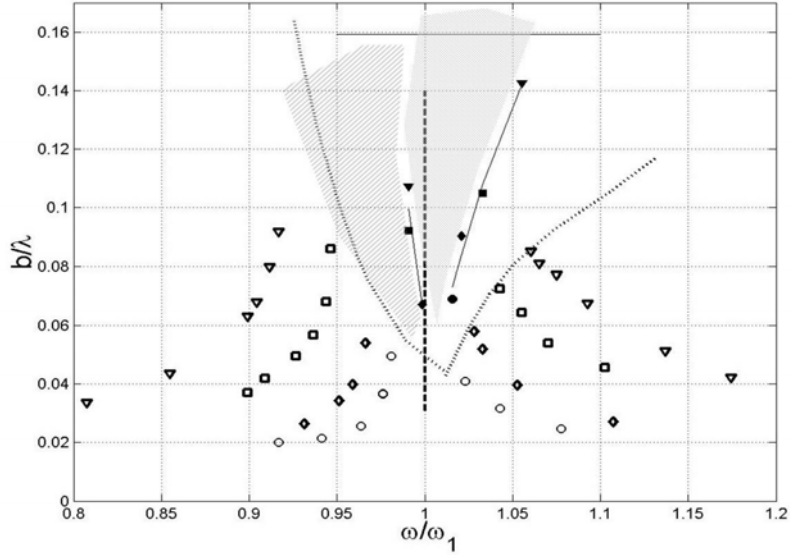


Figure 1: Amplitude-frequency diagram for four different forcing amplitudes A/R : ∇ , planar wave mode 1; \circ , swirling wave mode for $A/R = 0.0266$; \square , \circ , $A/R = 0.0133$; \diamond , \circ , $A/R = 0.0066$; \bullet , $A/R = 0.0033$. A stable swirling wave (dotted region) exists between the filled symbols and chaos to the left of it (hatched region). The dotted branches are the bounds of swirl of Abramson (1966). The upper horizontal line indicates $b\omega^2 = g$, giving $b/\lambda = 0.16$ ($\lambda = 3.411R$). The container, filled with water to $h/R \approx 1.5$, has a radius $R = 78$ mm.

When starting at $\omega/\omega_1 < 1$ and then increasing the forcing frequency by small increments, the planar wave amplitude, for a given forcing amplitude, increases with frequency until the wave amplitude reaches a turning point (point β_s of Miles' theory) and grows rapidly until wave breaking occurs. This regime is referred to as chaos (Miles 1984b, Faltinsen et al. 2003). The upper horizontal line in Figure 2 is the limit where the wave amplitude is such that the downward acceleration $b\omega^2$ is equal to gravity; this wave amplitude is referred to as b_c . Breaking requires $b \geq b_c$ (Taylor 1953). However, chaotic sloshing can occur without breaking; that is, without reaching amplitudes such that the downward wave crest acceleration equals gravity.

2.2.2 Phase diagram

A better representation of the bounds of steady-state wave motion and chaos is to plot the phase diagram, i.e. dimensionless forcing amplitude A/R as a function of ω/ω_1 . This is shown in Figure 2; the symbols are the same as in Figure 1. The relation between A/R and ω/ω_1 is given by the frequency-offset

parameter β and the bounds are given by the specific values of $\beta_2, \beta_3, \beta_4, \beta_5$ (or β_6) determined from Miles' (1984b) theory. For $\alpha^2 \ll 1$ and large fluid depth, $h/R > 1.5$, the bifurcation point β_1 does not exist and $\beta_2 = -0.36$. The other bifurcation points are to leading order (higher order terms are in α^2 and amount to less than 2% of the leading order terms) $\beta_3 = -1.55$, $\beta_4 = 0.735$, $\beta_5 = 0.108/\alpha^2$, $\beta_6 = 0.717$. In Figure 4 the lines corresponding to these bifurcation points are indicated. These lines are given by:

$$\frac{A_f}{R} = \frac{1}{1.684} \left[\frac{(\omega/\omega_1)^2 - 1}{\beta_i} \right]^{3/2} \quad (6)$$

where $i = 2, 3, 4, 5, 6$. The bifurcation point β_5 is clearly not physical. The values of these bifurcation points change with fluid depth when it is no longer asymptotically large, that is when $h/R < 1$. The values can be calculated from Miles' theory but there is no experimental support, especially for cases when h/R is in the neighborhood of the critical values $h/R = 0.506$ and $h/R = 0.15$.

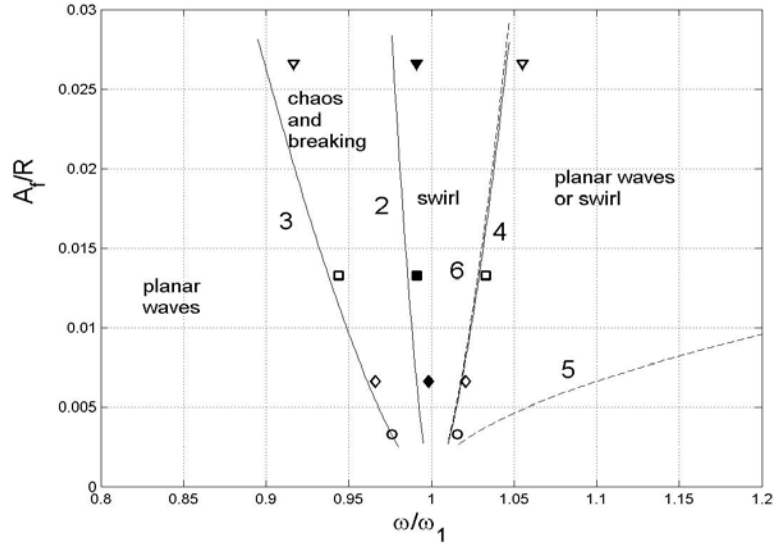


Figure 2: Phase diagram of dimensionless forcing amplitude A_f/R versus frequency ratio ω/ω_1 for four forcing amplitudes (see Figure 1 for symbols). The solid lines are the bounds where the number of fixed points changes, given by $\omega/\omega_1 = (\beta_i \varepsilon^2 + 1)^{1/2}$, $i = 2, 3, 4, 5, 6$. The bounds corresponding to the bifurcation points β_5 and β_6 are indicated by dashed lines.

2.2.3 Steady-state planar waves

Figure 2 indicates that the steady-state planar wave amplitude depends on forcing amplitude and forcing frequency. Linear oscillators would suggest

that $\frac{b}{A_f} = C_1 \frac{K^2}{|1-K^2|}$ where $K = \omega/\omega_1$. While for $\omega/\omega_1 < 1$ the data would collapse reasonably well by this scaling, this is not the case for $\omega/\omega_1 > 1$. The weakly nonlinear theory of Miles (1984b) predicts this asymmetry. The planar wave amplitude response curves terminate at the fixed points $\beta_3 = -1.55$, and $\beta_4 = 0.735$, giving respectively $\omega/\omega_1 = (-1.55\epsilon^2 + 1)^{1/2}$ and $\omega/\omega_1 = (0.735\epsilon^2 + 1)^{1/2}$. For the smallest excitation amplitude $A_f/R = 0.0033$ the corresponding values ω/ω_1 are 0.976 and 1.011.

The wave motion behaves like a damped oscillator with the superposition of two frequencies, namely ω and ω_1 when starting to force the container at a frequency $\omega = K\omega_1$ with $K \neq 1$; a strong beating is observed at a frequency $|\omega_1 - \omega|$. As expected, the amplitude of the natural frequency oscillation decays exponentially and is negligible after about 100 periods. The damping rate κ is given by $\kappa = \delta\omega_1$ where $\delta = C_1 \nu^{1/2} R^{-3/4} g^{-1/4}$, with $C_1 \approx 1$.

2.2.4 Swirling wave mode

The swirling wave mode also referred to as rotary sloshing by Ibrahim (2005) is observed when $\beta_2 < \beta < \beta_4$. Figure 3 shows images of a large amplitude ($b > 0.16\lambda$) swirling wave taken at 67 ms interval that corresponds to 0.12 wave periods. There are fairly large disturbances in the vicinity of the (flat-top) wave crest (local breaking) but the wave remains stable. Nonlinear waves can transfer angular momentum to the whole liquid column that starts to rotate (Faller 2001; Prandtl 1949). The result is a Doppler shift, causing the wave frequency to increase with respect to the forcing frequency. Because of the liquid rotation the swirl wave can be maintained up to fairly large forcing frequencies, here up to $\omega/\omega_1 \approx 1.3$, when the forcing frequency is increased by small increments. There is continuous local wave breaking near the wave crest but as long as the forcing frequency remains below the collapse frequency the swirl wave is maintained. When the forcing frequency is further increased by a small amount, the swirl wave suddenly collapses and the motion switches to a small amplitude, out of phase, planar wave motion.

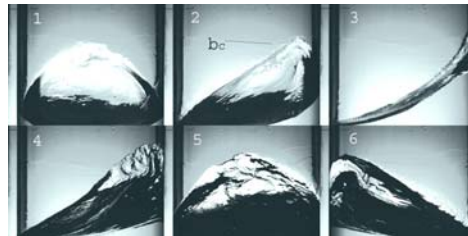


Figure 3: Images of swirling wave in circular cylinder of radius $R=150$ mm partially filled with water: Views are in the direction normal to the tank motion. The time between two images is 67 ms. The six images represent somewhat more than half a wave period $T = 2\pi/\omega = 570$ ms. $h/R \approx 1.2$, $\omega/\omega_1 \approx 1.02$, $A_f/R = 0.023$.

2.2.5. Chaotic sloshing and breaking conditions

Chaotic sloshing occurs when $\beta_3 < \beta < \beta_2$ (Figure 2). When the experiments are started at forcing frequencies below resonance and steady-state planar wave motion is established, a small increase in forcing frequency leads to a rapid increase in wave amplitude if the turning point β_3 is crossed. Rapid increase in wave amplitude and wave breaking occurs in a similar way in the whole range $\beta_3 < \beta < \beta_2$. The growth in wave amplitude near β_3 and wave breaking is illustrated in Figure 4a where the surface displacement is shown as a function of time, measured with the capacitance probe located at point $P1$ ($\theta = 0$). The surface displacement is made dimensionless by b_c and time by the forcing period $T = 2\pi/\omega$ (calculated with $\omega = 0.89\omega_1$). It is seen in Figure 4a that as the wave amplitude grows the motion gets more and more asymmetric with the positive, maximum surface displacements reaching nearly twice the negative displacements. The motion is initially in phase with the forcing but then the phase lag increases with wave amplitude (Figure 4b). When $b > b_c$ the phase lag increases rapidly to $-\pi/2$ and is $-\pi$ at collapse. After breaking of the planar wave, an irregular swirl is generated and when the irregular sloshing motion has decayed sufficiently, the planar wave grows again in amplitude until breaking. This behaviour occurs quasi-periodically.

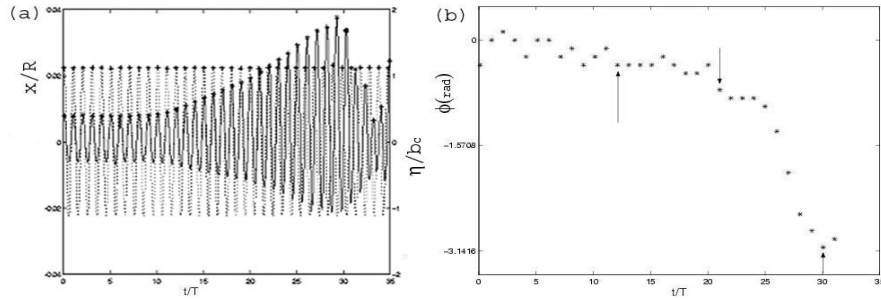


Figure 4: (a), time evolution of dimensionless wave amplitude b/b_c versus dimensionless time. (b), corresponding phase lag ϕ (rad). The forcing amplitude (left scale in a) is $A_f/R = 0.022$, $R = 150$ mm, $h/R = 1.5$. Up to $t/T=10$ the forcing amplitude was $\omega/\omega_1 = 0.89$, then it was increased to $\omega/\omega_1 = 0.92$. $T = 2\pi/\omega = 622$ and 640 ms, $b_c = 0.54R$.

The growth of the planar wave amplitude is to first approximation linear in time (Figure 4a) and nearly proportional to forcing amplitude in the form

$$\frac{b}{R} \approx C_2 \pi \left(\frac{A_f}{R} \right)^n \frac{t}{T} \quad (7)$$

Linear oscillator theory suggests $n = 1$. Taking this value of n the constant $C_2 = 0.3$ to 1.5 depending on initial conditions. In general, the growth rate was found to be larger when the wave amplitude in the chaotic regime grows from rest, whereas the growth rate is less in the case of an established planar wave motion with a following small forcing frequency increase to the chaotic regime, as shown in Figure 4. Miles theory would suggest $n = 2/3$, giving $d(b/R)/dt = 0.70C_2$, where $\tau = (\varepsilon^2 \omega t)/2$ is the slow dimensionless time scale in Miles' theory. For large wave amplitudes the weakly non-linear theory is no longer valid and the exponent may deviate from $n = 2/3$.

In the whole chaotic regime wave breaking and collapse show a similar behavior except that further away from the swirl wave boundary there is less or no regular swirl generated when the planar wave motion collapses. A layer moves up the wall and the crest is destabilized in the crosswise direction and two perturbations begin to grow at the edges of the layer. A period later, the pattern is repeated but is less regular. Therefore, the frequency of this cross-wave can be considered to be equal to twice the primary frequency ω_1 . In a square-base container, cross-waves of twice the primary wave frequency are indeed observed but other scenarios are also possible, as demonstrated by Royon-Lebeaud et al. (2007).

Before the violent wave destabilization (collapse), spilling occurs. This is shown in Figure 5 where a jet is seen in the two last rows. In 5a the motion is viewed perpendicular to the container motion and in Figure 5b aligned with the container motion. The two views are, unfortunately, not simultaneous. The mechanism of spilling is analogous to the one beautifully demonstrated by Jiang et al. (1998) for two-dimensional wave breaking except that in 3D, because of the crosswise wave crest destabilization, there is no period tripling.

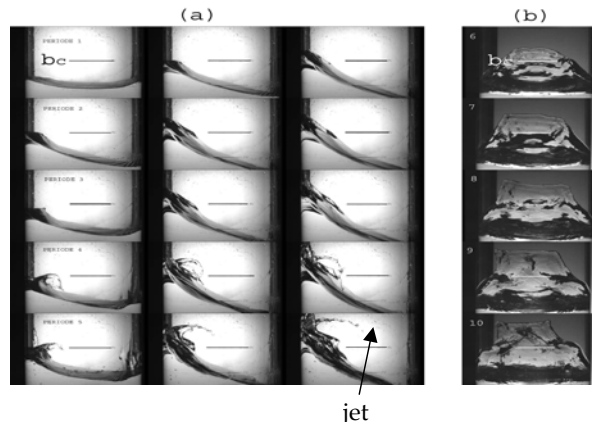


Figure 5: (a), Slashing motion viewed perpendicular to the container motion at successive periods. For each period three images with increasing wave amplitude are shown (b), view in the direction of container motion. Cylindrical container of $R = 78$ mm, filled with water to $h/R = 1.5$. The forcing frequency and forcing amplitude are respectively $\omega/\omega_1 = 0.96$ and $A_0/R = 0.022$. The wave period is $T = 430$ ms.

3. Impulsive Forcing and Axi-symmetric Slushing

An example of impulsive forcing after a micro-gravity phase is the falling coffee cup experiment by Milgram (1969). Baumbach et al. (2005) used membranes, simulating high surface tension, to obtain small, initial Bond numbers. Rupture of the membrane leads to a step increase in Bond number. It is possible to use a rigid barrier instead of a membrane. The sudden withdrawal of the barrier (infinite surface tension) is analogous to a step increase in acceleration after low gravity conditions, corresponding to a sudden increase in Bond number. These experiments are referred to as axi-symmetric dam-break experiments.

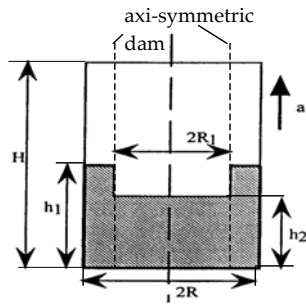


Figure 6: Schematic representation of the dam-break experiments. The initial state of the liquid, indicated by the shaded area, is maintained by the axi-symmetric barrier of outer radius R_1 in the container of radius R . The step change $\Delta h = h_1 - h_2$ of the free surface simulates the rise of the liquid near the container wall under low gravity conditions.

Figure 6 shows a schematic view of the dam-break experiments. The container, made of glass, has an inner diameter $2R = 296 \pm 2$ mm and depth 600 mm; the

error in verticality is 0.4° . The initial liquid column conditions are achieved by positioning a barrier (tube) of outer radius $R_1 = 100$ mm and 4 mm wall thickness at the center of the container. This tube is open on both ends and has a watertight contact with the tank bottom. The annular space of $d = R - R_1 = 48$ mm is filled with liquid (water or alcohol) to depth h_1 and the central space to depth h_2 . The important scale is $\Delta h = h_1 - h_2$. The three experimental conditions considered are: **Exp1**: $h_1 = 150$ mm, $h_2 = 0$; **Exp2**: $h_1 = 50$ mm, $h_2 = 0$; **Exp3**: $h_1 = 100$ mm, $h_2 = 50$ mm.

The experiments begin by removing suddenly the barrier (inner tube) of radius R_1 . It is crucial that the tube be removed sufficiently rapidly (with an acceleration $> 10g$) so that the fluid column has a negligible motion while the tube is withdrawn. The flow was determined by image processing. The images were taken at 500 Hz with a high-speed camera and a resolution of 0.322 mm per pixel for a 1536x1024 pixels matrix of the image.

3.2 Results

3.2.1 Geysier initiation and shape

In Figure 7 geysier initiation (right after the liquid front arrived at the centre) and maximum geysier heights and shapes are shown for the three experimental conditions. The first observation is that the maximum geysier height h_{gm} is considerably larger than Δh . The maximum height is given by

$$h_{gm} = U_{g0}^2/(2g) + h_2 . \quad (8)$$

This height is $h_{gm}/\Delta h \cong 5.3$ in **Exp1**, $h_{gm}/\Delta h \cong 14$ in **Exp2** and $h_{gm}/\Delta h \cong 9.4$ in **Exp3**. The overall conservation of mass and momentum would support the existence of a nearly cylindrical geysier of height equal to Δh (except for some overshoot) and of radius $R_g \cong \sqrt{2Rd(1-d/4R)}$. The radius of the geysiers at the base, shown in Figure 7, is close to this value but the shape is conical with the diameter decreasing rapidly with height, and then remains nearly constant at a value much less than R_g . The maximum geysier height corresponds to an initial geysier velocity, $U_{g0} = \sqrt{2gh_{gm}}$, that is much larger (by the factor $\sqrt{h_{gm}/\Delta h}$) than the maximum liquid column velocity $U_i = \sqrt{2g\Delta h}$. Momentum is transferred to only a small fraction of the liquid mass that is projected up to height h_{gm} but when this geysier collapses considerable gas entrainment into the liquid occurs (see Figure 9).

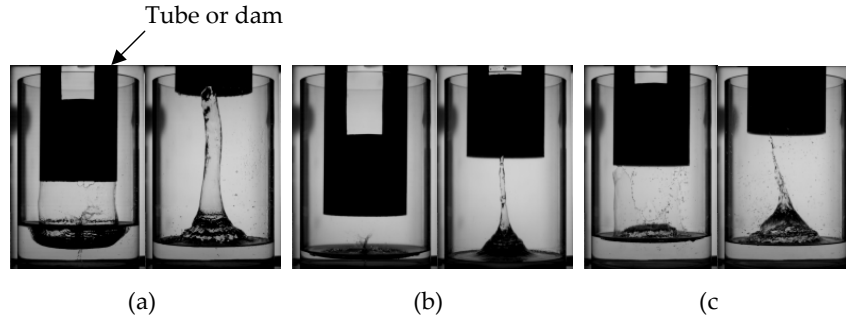


Figure 7: Geyser initiation and shape. (a), $h_1 = \Delta h = 15\text{cm}$ (**Exp1**), $t_1 = 0.05$ s (initiation) and $t_2 = 0.45$ s (maximum height of geyser); (b), $h_1 = \Delta h = 50$ mm (**Exp2**), $t_1 = 0.13$ s and $t_2 = 0.51$ s; (c), $h_1 = 100$ mm, $h_2 = 5\text{cm}$, $\Delta h = 50$ mm (**Exp3**), $t_1 = 0.14$ s and $t_2 = 0.41$ s. $t_f = \sqrt{2\Delta h/g} = 0.175$ s in exp 1 and 0.101s in exp 2 and 3. The scale in the images is given by the tube diameter equal to 200 mm.

The geyser diameter r_g above the conical base depends on the thickness of the front of the liquid layer when it arrives at the center. In Fig 7b the front remains thin and r_g is small but is at arrival an order of magnitude larger than the capillary scale $l_c = \sqrt{\sigma/\rho g}$. In Fig 7a the front is much thicker. The most likely reason for this is that the ratio of front acceleration time, equal to the time of collapse of the liquid column $t_f = \sqrt{2\Delta h/g}$, to radial propagation time $t_R = \sqrt{2R_1^2/g\Delta h}$ is 1.5 in exp 1 and 0.5 in exp 2.

3.2.2 Effect of a central liquid layer

Geyser formation in the presence of a central liquid layer (Exp 3) is similar to the falling cup experiment of Milgram (1969). Figure 7 indicates that the geyser height depends principally on Δh and of course on the acceleration applied to the container that is g in the present experiments (in Migram's experiments it is dV/dt , where V is the container velocity at impact). The geyser evolution (its height and diameter) in Figure 7c is close to that of Figure 7b. However, the geyser initiation is different. This initiation is clearly demonstrated by numerical simulations shown in Figure 8b (courtesy of Jean-Paul Vila, ONERA). When the initial step change in interface height is suddenly released a surface wave starts to propagate toward the center and an annular front forms (Figure 8b) that accelerates and merges at the center. This is referred to as flip-through (private communications D.H.Peregrine) encountered when a surface wave approaches a wall. In the experiments (Figure 8a) only the envelope of this front is seen.

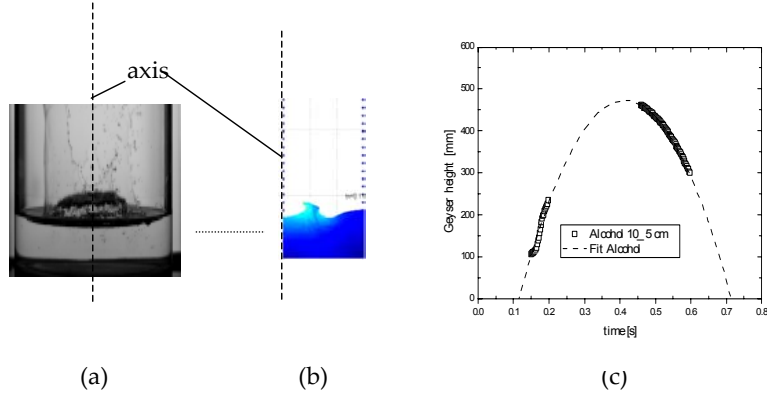


Figure 8: Geysers evolution in exp 3. (a), image just before geysers appearance. (b), numerical simulations (J.-P. Vila) showing the flip-through. (c), geysers height as a function of time.

3.2.3 Sloshing motion

After collapse of the geysers a second, smaller geysers emerges and then, smaller and smaller geysers until the liquid sloshing has been damped. This sloshing motion consists of a symmetric, non-linear wave mode as shown in figure 9 for conditions of exp 3 and respectively for water (Figure 9a) and alcohol (Figure 9b). The difference between water and alcohol is the surface tension resulting, for the same experimental conditions, in a larger Bond and Weber number in the case of alcohol. Hence, smaller drops and bubbles associated with breaking of the geysers top and gas entrainment on geysers collapse appear. The relevant Weber number is $We = \frac{\rho U_{g0}^2 r_g}{\sigma}$ which gives together with $U_{g0} = \sqrt{h_{gm} / \Delta h} U_l$ and $r_g \sim R_g \Delta h / R$ a characteristic Bond number $Bo = \frac{\rho g \Delta h^2}{\sigma} \sqrt{\frac{d}{R}} \frac{h_{gm}}{\Delta h}$. This Bond number is $> 10^3$ in all the experiments.

The alcohol experiments have a larger Bond number and it is seen in Figure 9 that the second, third and following geysers are more irregular (Figure 9b) and drops are smaller and more gas is entrained or at least it remains in the liquid layer for a longer time.

The time interval between the images shown in Figure 9a is close to $T \approx 400$ ms that corresponds to a frequency $\omega = 2\pi/T \approx 15.7$ rad/s. The dispersion relation $\omega^2 = kg \tanh(kh_l)$, where h_l is the fluid layer depth and $k = 3.83/R$ the wave number for the first symmetric mode, gives $\omega = 15.5$ rad/s. For alcohol the second third and fourth geysers are shown in Figure 9b. The time interval is again $T \approx 400$ ms that is to be expected.

The decay of the sloshing motion is exponential, of the form $A=A_0 \exp(-\gamma \omega t)$. A_0 is the amplitude of the second geyser, first image in Figure 9a and b. The initial decay of geyser amplitude is large, $\gamma \approx 0.023$ because the liquid layer is very agitated (probably turbulent). Then the decay is considerably slower, $\gamma \approx 0.0073$. Dissipation is at the boundaries of the container (side and bottom) and internal in the beginning and then only at the boundaries. The parameter γ is given by $\gamma = C(v^2/R^3g)^{1/2}$ with the constant C being about 16 in the beginning and 3 for the decay after the second or third geyser.



Figure 9: Decay of sloshing motion in exp3. (a), water, (b), alcohol. The images are taken at 400 ms interval

4. Conclusions

The experimental results on asymmetric sloshing cover a wide range of forcing frequencies and forcing amplitudes in the asymptotic limit of large fluid depth and low viscosity liquids. The bounds of existence of the different wave amplitude responses are clearly established, namely planar waves, swirling waves and breaking waves. In the chaotic regime wave breaking occurs quasi periodically: growth of planar wave amplitude, collapse, irregular swirl and again growth of planar wave amplitude. It is shown that asymmetric sloshing is controlled by three non-dimensional (similarity) parameters that are the liquid depth parameter, the frequency offset (depending on forcing frequency and forcing amplitude) and the damping parameter in agreement with Miles (1984b) theory. This theory contains a small parameter, $\varepsilon \ll 1$. Experiments show that the theory remains valid to leading order when ε is in the range up to 0.5. Surface tension effects on the tank scale are assumed to be negligible (Bond number $Bo = \frac{\rho g R^2}{\sigma} \gg 1$). Surface tension effects play a role in the final stage of wave breaking (drop formation).

The results of the dam-break experiments show that when a relatively small change in surface height is subjected to a step change an axial acceleration, a phenomenon called flip-through occurs. This leads to intense geyser

formation, followed by violent sloshing with gas entrainment. This situation is encountered on engine restart after a micro-gravity phase.

Acknowledgements

This work was financially supported by contracts CNES n° 5866 and n° 1616 within the frame of the French-German program COMPERE.

References

- [1] Abramson, H.N. 1966 The dynamic behavior of liquids in moving containers. NASA Technical Report SP-106.
- [2] Baumbach, V., Hopfinger, E.J. and Cartellier, A. 2005 The transient behaviour of a large bubble in a vertical tube. *J. Fluid Mech.* **524**, 131-142
- [3] Faller, A.J. 2001 The constant-V vortex. *J. Fluid Mech.*, **434**, 167-180.
- [4] Faltinsen, O.M., Rognebakke, O.F. and Timokha, A.N. 2003 Resonant three-dimensional nonlinear sloshing in a square basin. *J. Fluid Mech.*, **487**, 1-42.
- [5] Funakoshi, M. and Inoue, S. 1988 Surface waves due to resonant horizontal oscillations. *J. Fluid Mech.* **192**, 219-247
- [6] Ibrahim, R.A. 2005 *Liquid Sloshing Dynamics*. Cambridge University Press.
- [7] Jiang, L., Perlin, M. and Schultz, W.W. 1998 Period tripling and energy dissipation of breaking standing waves. *J. Fluid Mech.*, **369**, 273-299.
- [8] Miles, J. W. 1984a Internally resonant surface waves in a circular cylinder. *J. Fluid Mech.*, **149**, 1-14.
- [9] Miles, J. W. 1984b Resonantly forced surface waves in a circular cylinder. *J. Fluid Mech.*, **149**, 15-31.
- [10] Milgram, J. H. 1969 The motion of a fluid in a cylindrical container with a free surface following vertical impact. *J. Fluid Mech.* **37**, 435-448
- [11] Prandtl, L. 1949 Erzeugung von Zirkulationen beim Schütten von Gefassen. *Z. Angew. Math Mech.* **29**, 8-9.
- [12] Royon-Lebeaud, A., Hopfinger, E. J. and Cartellier, A. 2007 Liquid sloshing and wave breaking in circular and square-base cylindrical containers. *J. Fluid Mech.* (in press).
- [13] Taylor, G.I. 1953 An experimental study of standing waves. *Phil. Trans. Roy. Soc.*, CCXVIII, 44-59.
- [14] Waterhouse, D.D. 1994 Resonant sloshing near a critical depth. *J. Fluid Mech.*, **281**, 313-318.

EUROMECH Young Scientist Prize Paper

“Generation of Prescribed Extensional Waves in an Elastic Bar by Use of Piezoelectric Actuators”

Anders Jansson won the EUROMECH Young Scientist Prize, awarded at the sixth EUROMECH Solid Mechanics Conference held in Budapest, August 2006

A. Jansson¹, U. Valdek² and B. Lundberg³

Abstract

A symmetrically attached piezoelectric actuator pair, driven by a linear power amplifier, was used to generate a prescribed extensional wave in an aluminium bar. The strains in the bar were measured by use of semiconductor strain gauges. Theoretical results for a general amplifier were specialized to those for an ideal amplifier with voltage gain real and constant and output impedance zero. These results, in the form of time-domain difference and difference-differential equations, were used to determine the required input voltage to the amplifier. A fair agreement was found between the experimental and theoretical results. The simplicity of the latter makes them useful in control applications.

1. Introduction

Piezoelectric elements are used as actuators and sensors in various applications [1-4]. The main reason for this is their ability to produce electrical response to mechanical stimuli and vice versa. These properties are described by two coupled constitutive relations [5] relating the mechanical and electrical properties of the piezoelectric material. Due to their relatively large bandwidth, piezoelectric elements are well suited for applications involving generation and sensing of mechanical waves. Crawly and de Luis [6] utilized the actuator properties in their pioneering study of the interaction between surface-mounted piezoelectric actuators and an Euler-Bernoulli beam.

When piezoelectric elements constitute integral parts of mechanical structures, their effective mechanical properties are influenced by the presence of external electrical circuits. Correspondingly, their electrical properties are influenced by the presence of the mechanical structure [7]. In real-time control involving mechanical waves, however, models which take into account every aspect of

The Ångström Laboratory, Uppsala University, Box 534, SE-751 21 Uppsala, Sweden

¹ E-mail: anders.jansson@angstrom.uu.se

² E-mail: urmas.valdek@angstrom.uu.se

³ E-mail: bengt.lundberg@angstrom.uu.se

the interaction between the electrical circuits, the piezoelectric elements and the structure are often not workable because of their excessive demands on computational speed. Consider for example a system described by Fuller [8] and analyzed by Nauc ler et al. [9], which is aimed to reverse the direction and amplitude of mechanical waves travelling in a bar, much like a reflecting free boundary. On the basis of input from sensors, a controller should calculate the necessary input signal to a power amplifier driving actuators. Due to the rapidity of the wave phenomena involved, it may be impossible to implement such a controller unless the behaviour of the electromechanical system can be represented by a relatively simple model with sufficient accuracy.

The aim of this paper is to formulate simple time domain relations, well suited for implementation in real-time controllers, which describe the process of extensional wave generation in a linearly elastic bar by use of piezoelectric actuators. The aim is also to produce a prescribed extensional wave in an aluminium bar by use of these relations.

2. Theory

Consider a pair of piezoelectric actuator plates with rectangular cross-sections which are symmetrically mounted on the surface of a long linearly elastic bar with rectangular cross-section as shown in Fig. 1. The actuators are driven in phase by an ideal linear power amplifier with constant and real gain and zero output impedance. Furthermore, the actuators are considered to be lossless, and the influence of bonding layers between them and the bar is neglected.

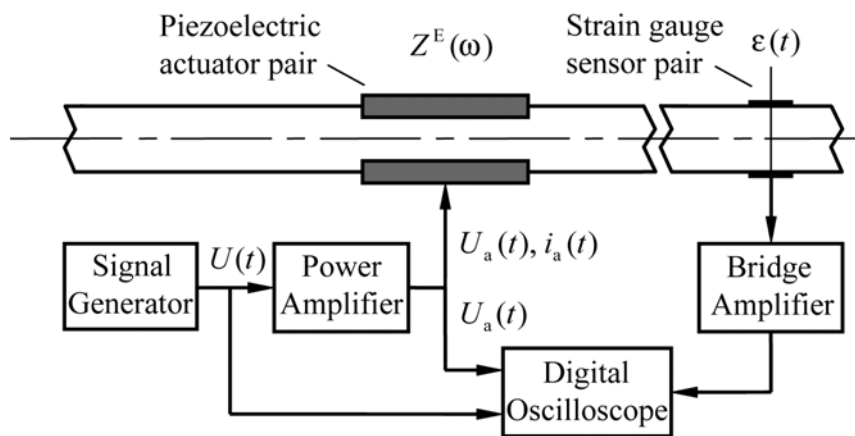


Figure 1: Electromechanical system for generation of extensional waves in an elastic bar.

It is assumed that plane cross-sections remain plane, and the stress is uni-axial. Outside the actuator region, the bar is characterized by its cross-sectional area A , Young's modulus E and density ρ . The speed of extensional waves in this region is $c = (E/\rho)^{1/2}$, and the mechanical impedance is $Z^M = AE/c$. Within the actuator region, the cross-sectional area of the bar is reduced to A_c . The actuators have cross-sectional area A_a , short-circuited Young's modulus E_a and density ρ_a . Effectively, the laminated actuator region is characterized by the cross-sectional area $A_0 = 2A_a + A_c$, density $\rho_0 = (2A_a\rho_a + A_c\rho)/A_0$ and Young's modulus $E_0 = (2A_aE_a + A_cE)/A_0$. Therefore, the speed of extensional waves in this region is $c_0 = (E_0/\rho_0)^{1/2}$, and the mechanical impedance is $Z_0^M = A_0E_0/c_0$. The piezoelectric material is characterized also by its permittivity ε_a and the absolute value d_a of its piezoelectric coefficient. The piezoelectric coupling coefficient is $k^2 = d_a^2E_a/\varepsilon_a$, and each piezoelectric actuator plate has the capacitance $C_a = \varepsilon_a l_a w_a / h_a$, where l_a is the length and w_a the width.

The output voltage of the amplifier is

$$U_a(t) = G_0 U(t), \quad (1)$$

where $U(t)$ is the input voltage and G_0 is the constant voltage gain. The output current is

$$\hat{i}_a(\omega) = \frac{\hat{U}_a(\omega)}{Z^E(\omega)}, \quad (2)$$

where $Z^E(\omega)$ is the electrical impedance of the actuator-bar assembly loading the amplifier, ω is the angular frequency, and top hat indicates Fourier transform. This impedance is [7]

$$Z^E(\omega) = \frac{Z_0^E(\omega)}{1 - k^2(1 - 4F(\omega)Z_a^M(\omega)/Z^M)} \quad (3)$$

with

$$F(\omega) = \frac{1 - e^{-i\omega t_a}}{p - qe^{-i\omega t_a}}, \quad p = \left(1 + \frac{Z_0^M}{Z^M}\right), \quad q = \left(1 - \frac{Z_0^M}{Z^M}\right), \quad (4a-c)$$

where $Z_0^E(\omega) = 1/i\omega 2C_a$, $Z_a^M(\omega) = A_a E_a / i\omega l_a$, and $t_a = l_a / c_0$ is the wave transit time through the actuator region.

The strain generated in the bar at each end of the actuator region is [7]

$$\hat{\varepsilon}(\omega) = 2 \frac{A_a E_a d_a}{AE h_a} F(\omega) \hat{U}_a(\omega). \quad (5)$$

Inverse Fourier transformation of equations (1-5) give the time-domain difference equations

$$\begin{aligned} i_a(t) = & \frac{q}{p} i_a(t-t_a) + 2(1-k^2) C_a G_0 \left[\frac{dU}{dt}(t) - \frac{q}{p} \frac{dU}{dt}(t-t_a) \right] + \\ & + 8k^2 C_a G_0 \frac{A_a E_a}{t_a c_0} \frac{1}{Z^M + Z_0^M} [U(t) - U(t-t_a)] \end{aligned} \quad (6)$$

and

$$\varepsilon(t) = \frac{q}{p} \varepsilon(t-t_a) + 2 \frac{A_a E_a d_a}{AE h_a} \frac{1}{p} G_0 [U(t) - U(t-t_a)] \quad (7a)$$

for the output current $i_a(t)$ and the strain $\varepsilon(t)$, respectively, in terms of the input voltage $U(t)$ to the amplifier. The inverse relation

$$U(t) = U(t-t_a) + \frac{1}{2} p \frac{AE h_a}{A_a E_a d_a} \frac{1}{G_0} \left[\varepsilon(t) - \frac{q}{p} \varepsilon(t-t_a) \right] \quad (7b)$$

of equation (7a) gives the required input to the amplifier in terms of the strain associated with a prescribed wave.

3. Experiment

An aluminium bar with length 2.80 m and square cross-section with area $A = 16 \text{ mm}^2$ was suspended vertically, clamped at its upper end and free at its lower end. The length of the actuator region was $l_a = 95.4 \text{ mm}$, and the upper end of the actuator region was located 950 mm from the clamped upper end of the bar. With the aim to achieve approximate impedance matching between the outer parts of the bar and the actuator region, the bar was milled in the actuator region so that a rectangular cross section with reduced area $A_c = 1.02 \times 4 = 4.08 \text{ mm}^2$ was obtained. In order to avoid bending, care was taken not to change the axis of symmetry of the bar. The material of the bar was characterized by its Young's modulus $E = 69 \text{ GPa}$ and density $\rho = 2700 \text{ kg/m}^3$.

Within the milled section of the bar, three piezoelectric plates (Piezo Systems, Inc., T226-A4-203Y, ceramic type 5A4E) with length 31.8 mm and rectangular cross-section with area $A_a = 0.66 \times 6.4 = 4.22 \text{ mm}^2$ were attached symmetrically on each side by use of thin layers of industrial epoxy. On each side, the three piezoelectric plates were connected electrically in parallel so that they would act as a single actuator with total length $3 \times 31.8 = 95.4 \text{ mm}$. Each such plate was characterized by the short-circuited Young's modulus $E_a = 66 \text{ GPa}$, the density $\rho_a = 7800 \text{ kg/m}^3$, the absolute value of piezoelectric constant $d_a = 190 \cdot 10^{-12} \text{ m/V}$, the piezoelectric coupling coefficient $k^2 = 0.15$, the capacitance $C_a = 14.8 \text{ nF}$ and the height $h_a = 0.66 \text{ mm}$.

The bar was instrumented with a pair of semi-conductor strain gauges (Kyowa, type KSP-2-120-E3) located 800 mm from the lower end of the actuator region. This relatively long distance was chosen in order to ensure that the strain gauges would not pick up electromagnetic noise from the excitation of the actuators. The strain gauges were connected to bridge amplifiers (Vishay Measurements Group, 2210).

A power amplifier (Piezo Systems, Inc., EPA-104) was used to drive the actuators in parallel. Due to its current constraint, it was linear only if $|i_a(t)|_{\max} < 200 \text{ mA}$. The DC voltage gain of the unloaded amplifier was measured to be 11.9. The input signal to the amplifier was generated by a computer-based signal generation card (Adlink Technology, Inc., DAQ-2010). Before there was any influence of waves reflected from the ends of the bar, the input voltage to the amplifier, the output voltage from the amplifier and the strains were recorded by means of a computer-based digital oscilloscope card (Strategic Test AB., UF.3122).

The wave to be generated was defined by the single-period sine pulse

$$\varepsilon(t) = \varepsilon_{\text{amp}} \sin(\pi t/t_a) [\theta(t) - \theta(t - 2t_a)], \quad (8)$$

where $2t_a$ is the duration, ε_{amp} is the amplitude and $\theta(t)$ is the Heaviside unit step function. The input voltage to the amplifier required to generate this pulse was determined from equation (7b), and the corresponding output current of the ideal power amplifier, without current constraint, was determined from equation (6).

4. Results and discussion

From the dimensions and material properties of the actuator-bar assembly, some characteristic parameters were obtained as follows. The wave speeds in

the bar and actuator regions were $c = 5050$ m/s and $c_0 = 3300$ m/s, respectively, and the transit time for a wave through the actuator region was $t_a = 28.9$ μ s. The characteristic mechanical impedances in the bar and the actuator region were $Z^M = 219$ Ns/m and $Z_0^M = 254$ Ns/m, respectively. The reflection coefficient $(Z^M - Z_0^M)/(Z^M + Z_0^M) = -0.075$ and transmission coefficient $2Z^M/(Z^M + Z_0^M) = 0.925$ show that the system was not far from being impedance matched.

The theoretical and experimental results are shown and compared in Fig. 2. The theoretical input voltage to the amplifier, required for generation of the prescribed wave, is shown in Fig. 2 (a) together with the corresponding recorded input voltage. Similarly, the theoretical out-put voltage is shown in Fig. 2 (b) together with the corresponding recorded output voltage.

Fig. 2 (c) shows that the theoretically expected output current from the amplifier somewhat exceeds the current constraint of 200 mA. The experimentally generated strain is shown in Fig. 2 (d) together with the prescribed strain shifted in time 158 μ s. This shift corresponds to the wave speed in the bar and the distance between strain gauges and the end of the actuator region.

The spectrum of the theoretical input voltage to the amplifier is shown in Fig. 2 (e). It shows that frequencies up to 50 or 100 kHz were significant in the wave generation test. At these frequencies, the waves generated in the aluminium bar had wavelength $\lambda = c/f \approx 100$ mm and 50 mm, respectively. This is much more than the transverse dimension 4 mm of the bar, and therefore the one-dimensional model used for the actuator-bar assembly can be expected to be accurate [10].

In [11], the gain and output impedance of the amplifier used in this study were identified. The 3 dB cut-off frequency of the unloaded amplifier was found to be about 105 kHz. The output impedance was found to be resistive in nature with a dominating real part of 7.9 Ω and a small imaginary part corresponding to an inductance of about 3 μ H. In the frequency range of the test, therefore, the magnitude of the output impedance of the amplifier was generally small compared with the that of the loading impedance Z^E (130 Ω at 50 kHz and 60 Ω at 100 kHz) of the actuator-bar assembly. This justifies the assumption of an ideal amplifier with constant gain and zero output impedance.

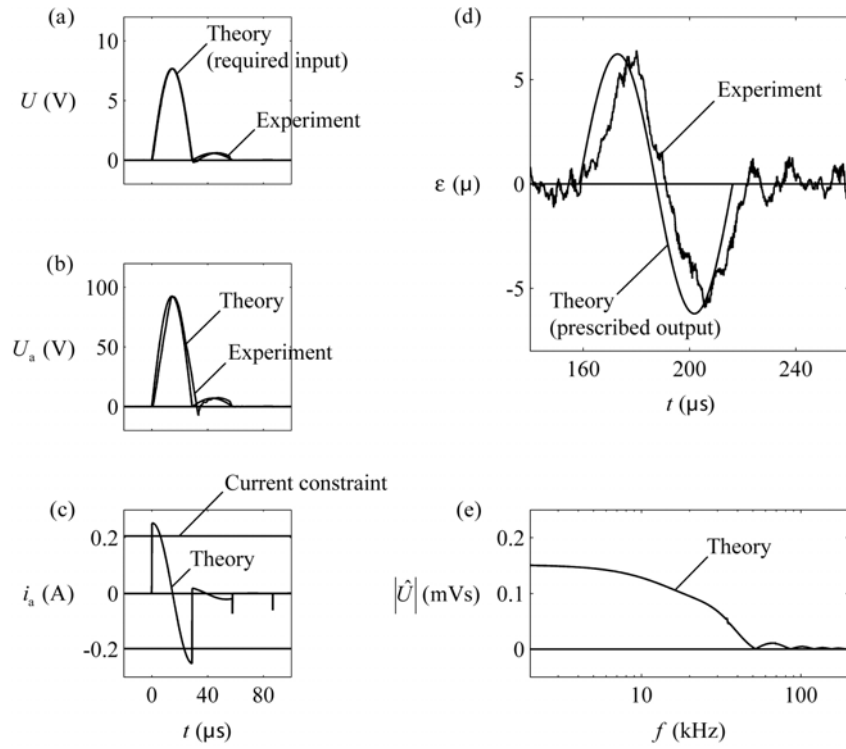


Figure 2. Generation of a prescribed wave associated with a single-period sine strain pulse.

The relatively small difference between the recorded and prescribed strain pulses in Fig. 2 (d) is found to be due mainly to the noise at the low signal level used and to the output current constraint of the amplifier. Equations (3) and (4) show that the impedance Z^E loading the amplifier is mainly of a capacitive nature. Therefore, the output current from the amplifier is approximately proportional to the time rate of change of the output voltage, which means that the output current constraint corresponds to a critical time derivative or slope of the output voltage shown in Fig. 2 (b).

5. Conclusions

The main conclusions of this study are as follows: (i) The ideal amplifier model can be used in a frequency range where the voltage gain, in the absence of load, is nearly constant and real, and where the magnitude of the output impedance is small compared with that of the impedance of the load constituted by the actuator-bar assembly. Furthermore, the output current constraint must not be exceeded. (ii) For an ideal amplifier and an elastic bar, the relations between the input voltage to the amplifier and the output strain associated with generated waves take the form of time-domain difference equations. (iii) Similarly, the output current and the input voltage of the ideal amplifier are related by time-domain difference-differential equations. (iv) A fair agreement was found between the experimental and theoretical results. (v) Because of its simplicity, the model of the electromechanical system should have use in real-time control applications with high demands on computational speed.

Acknowledgement

Financial support from the Swedish Research Council (Contract no 621-2001-2156) is gratefully acknowledged.

References

- [1] G.Gautschi, *Piezoelectric Sensorics*, Springer-Verlag, Berlin/Heidelberg, 2002.
- [2] R.Puers, W.Claes, W.Sansen, M.De Cooman, J.Duyck,I.Naert, Towards the limits in detecting low-level strain with multiple piezo-resistive sensors. *Sensors and Actuators A (Physical)* **85** (2000) 395-401.
- [3] J.K.Dürr, R.Honke, M.von Alberti, R.Sippel, Development of an adaptive lightweight mirror for space application. *Smart Materials and Structures* **12** (2003) 1005-1016
- [4] K.K.Tan, S.C.Ng, S.N.Huang, Assisted reproduction system using piezo actuator. *2004 International Conference on Communications, Circuits and Systems (IEEE Cat. No.04EX914)*, 2004, pt. 2, p 1200-3 Vol.2.
- [5] T.Ikeda, *Fundamentals of piezoelectricity*, Oxford University Press, New York, 1990.
- [6] E.F.Crawley, J.de Luis, Use of piezoelectric actuators as elements of intelligent structures. *AIAA Journal* **25** (10) (1987) 1373-1385.
- [7] A.Jansson, B.Lundberg, Piezoelectric generation of extensional waves in a viscoelastic bar by use of a linear power amplifier: theoretical basis. *Journal of Sound and Vibration*. Submitted for publication (2006).

- [8] C.R.Fuller, S.J.Elliott, P.A.Nelson, *Active Control of Vibration*, Academic Press Limited, London, 1996.
- [9] P.Naoclér, B.Lundberg, T.Söderström. A mechanical wave diode: Using feedforward control for one-way transmission of elastic extensional waves. *IEEE Transactions on Control Systems Technology* **15** (3). In press (2007).
- [10] H.Kolsky, *Stress waves in solids*, Dover Publications, Inc., New York, 1963.
- [11] A.Jansson, U.Valdek, B.Lundberg, Generation of prescribed strain waves in an elastic bar by use of piezoelectric actuators driven by a linear power amplifier. *Journal of Sound and Vibration*. Submitted for publication (2007).

EUROMECH Fluid Mechanics Fellow 2006 Paper

“Transition to Turbulence in Pipe Flow”

Bruno Eckhardt was named Fellow of EUROMECH at the sixth EUROMECH Fluid Mechanics Conference held in Stockholm, June 2006

B. Eckhardt

Fachbereich Physik, Philipps-Universität Marburg, 35032 Marburg

Many introductory textbooks in fluid mechanics and physics mention the transition to turbulence in pipe flow and assign a critical Reynolds number of about 2000 to it. The experiment is reasonably easy to set up and part of many undergraduate labs, so that the textbook description is seemingly confirmed by generations of students worldwide. This version of the story, however, misses many of the fascinating subtleties and surprising features revealed by closer inspection. One discovers, for instance, that there is no linear instability of the laminar profile, so that it not only exists at all Reynolds numbers, but is also stable against sufficiently small perturbations. Therefore, it should be possible to maintain the parabolic Hagen-Poiseuille profile at arbitrary flow speed (and hence to transport fluid with very low pressure differences), and indeed there are reports that by carefully eliminating perturbations in the inflow region it has been kept laminar up to Reynolds numbers of about 100.000. Next, one can be puzzled by the wide range of critical Reynolds numbers, which go from about 1700 to well above 2200. Because of this linear stability, finite amplitude perturbations are required to trigger turbulence, but the experiments show a remarkable sensitivity to details of perturbations, making it difficult to pin down an accurate threshold. Last but not least, when turbulence seems fully established, it can be observed to decay after some time without any discernable external influence. Similar features are observed for the linear shear flow between parallel plates and, with a minor variation, in pressure driven flow between parallel plates.

Over the last decade or so a framework has been developed that holds the promise that the different pieces of the puzzle fit together. It has been developed against the backdrop of phenomena seen in low-dimensional dynamical systems. Transient chaos, strange saddles, Smale horseshoes, hyperbolic tangles, periodic orbit theory and Markov chains are some of the technical terms which are deeply rooted in dynamical systems theory and which can be put to good use here. For some, the extension to the higher-dimensional cases relevant for flows is obvious, for others we are pushing the limits of what is mathematically established. But rather than going through

the technicalities, I here want to focus on key aspects that have emerged and which are most easily transferred to other situations.

When a fluid flow is approached from the dynamical systems point of view, the challenge is to understand its evolution in state space [1, 2, 3]. The state space for a fluid flow contains all (in the incompressible case: divergence-free) velocity fields that satisfy the boundary conditions. They evolve in time according to the Navier-Stokes equation and thereby trace out a trajectory in state space. Flows like the laminar Hagen-Poiseuille profile in pipe flow do not change in time and correspond to fixed points in this space. If such a state is linearly stable, then all sufficiently small perturbations decay and the flow relax towards it. In the sketch in Fig. 1, the open circle in the centre represents the laminar profile and the arrows pointing towards it indicate the linear stability.

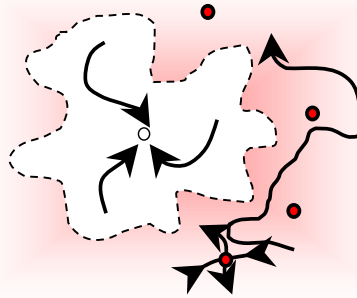


Figure 1: Sketch of the state space of pipe flow.

For turbulence to exist, the system has to have other solutions, indicated by the filled dots in the diagram. In their simplest form, they are coherent structures which are stationary, or travelling wave, or in other ways periodic. They cannot be stable, for otherwise they would stand out very much as the rolls in Rayleigh-Benard or Taylor-Couette, so they correspond to saddles, with stable directions along which the flow can evolve towards them, and unstable ones, along which it can depart. The unsteady dynamics of the turbulent state suggests that these stable and unstable directions are linked to form the support of the turbulent dynamics in state space. This is indicated by further arrows and the shading.

Finally, it is obvious that with laminar and turbulent dynamics coexisting for the same Reynolds number there has to be some kind of border between them, indicated in a very simplistic version by the dashed line.

In the following, I will focus on three aspects of this sketch: (i) the 3-d coherent structures around which the turbulence develops, (ii) a method that allows tracking the boundary between the laminar and the turbulent and (iii) the question of whether there are connections between the turbulent and laminar states that would indicate that the turbulence is transient only. Other aspects, such as the non-normal amplification near the laminar profile and its consequences for the sensitivity of the laminar profile to perturbations [4,5,6], the self-sustaining cycle for near wall structures as well [7], or all aspects having to deal with the spatial extension and the puff and slug structures seen in transitional flow, will have to be taken up elsewhere. References will be limited to a minimum, with a more complete set available in the review [8].

3-d structures

The basic tenet here is that there can be no turbulence unless there exist some more or less simple structures around which it can develop. In flows with linear instabilities, such as fluids heated from below or between rotating cylinders, these structures appear at the point of bifurcation in the form of coherent convection cells or Taylor vortices. As the driving force increases, more and more bifurcations give rise to structures with an increasing spatial and temporal complexity. But there is no example of a chaotic or turbulent flow without them. Therefore, it is a natural conclusion to expect similarly simple structures in pipe flow. Finding them with a direct search starting from velocity fields appearing in the time evolution of the flow has turned out to be next to impossible. However, when embedded in a larger family of flows, the structures can be stable for some parameters and, once found, can be tracked to the situation of interest [9,10]. The flow fields that have been identified so far have a fairly high degree of symmetry (which reduces the degrees of freedom and helps the search for the states), but more complicated ones as well as non-symmetric ones surely exist as well. All states are of the form of travelling waves, i.e. structures which drift downstream with a constant speed without changing their shape. They are dominated by downstream vortices, as shown in Fig. 2.

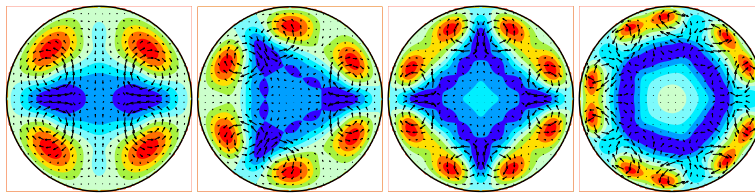


Figure 2: Velocity fields for coherent travelling waves in pipe flow, obtained by averaging over one period in the downstream direction. Arrows are the velocity components in the plane, the shading indicates the deviations of the downstream velocity component from a parabolic profile. From [9].

As expected, all these structures turn out to have unstable directions. This is consistent with the fact that they have not been observed as permanent flow structures. So what are the chances of identifying them in the flow? Calculations with 1-d chaotic maps sometimes show time traces which suggest that the trajectory gets close to a fixed point, stays nearby for a while and only then continues on its chaotic track. The probability for these events is controlled by the instability of the orbit, which determines its relative weight [11]. Similar things can happen in the full flow, where the flow during its time evolution comes close to one of the coherent states for a while. A striking example (obtained without any fine tuning of the parameters or initial conditions!) is shown in Fig. 3. These transient approaches are the basis on which the experimental identification builds [12]. Statistical analyses show such events to occur at about 20% of the times near Reynolds numbers of about 2000 [13].

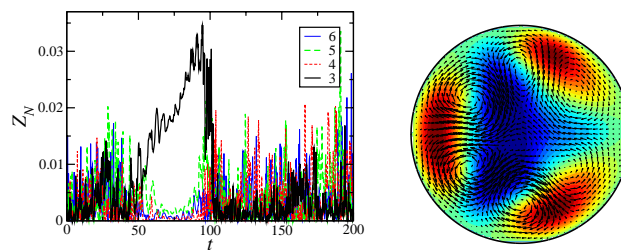


Figure 3: Transient appearance of a coherent travelling wave during the time evolution of turbulent flow field in a DNS simulation in a pipe of $5D$ length. The state was identified using indicator functions for N -fold symmetries in the flow (called Z_N). In the regular turbulent flow they fluctuated wildly, but as soon as the coherent state on the left is approached, Z_3 stands out and the others become very small.

Thus far, no such coherent structures have been found for Reynolds numbers below 1250. Is this then indeed the lowest possible? We do not know for sure and various examples tell us that we should be cautious. The fields discussed

have a high degree of symmetry and contain at least four pairs of vortices. Allowing for asymmetries gives more freedom and might result in vortex arrangements that could be more effective in exploiting the driving and could go lower in Reynolds number. The behaviour of fully time-dependent periodic orbits is even more difficult to gauge. In low-dimensional models we have studied periodic orbits come in first, well below the stationary states [14]. So we do not know whether 1250 is more than the lowest Reynolds number for which coherent states have been found thus far. Energy stability shows that all perturbations decay at Reynolds numbers below about 80: the true bound therefore is between 80 and 1250. The reader will surely have noticed that the coherent states appear at Reynolds numbers below the ones where experiments see evidence for turbulence: this observation awaits its explanation!

Transition states

When a laminar and a turbulent state coexist there must be some kind of border between them. Rather than starting from guesses as to which states could be in the border, we use an operational approach based on the comparison between two trajectories [15,16]: one that relaxes towards the laminar profile, and one that swings up to the turbulence. Even if they are initially close, they will separate in energy. Once the distance gets too large, one can pick a new pair with energies intermediate between the current ones and hence obtain an approximation to a trajectory that stays forever between laminar and turbulent. If it can neither become laminar nor turbulent, what can it do? As it turns out, it stays between the two extremes and evolves towards a flow that is dominated by a single pair of vortices. Different initial conditions approach the same structures (up to obvious symmetries), so that we are dealing with a relative attractor: attractor, because all states intermediate between turbulent and laminar evolve towards it, and relative because it is attracting only in this subset, and unstable against perturbations that increase or decrease its energy content.

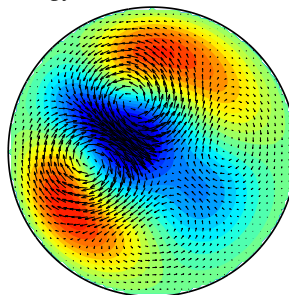


Figure 4: Snap shot of the edge state in pipe flow.

The significance of this relative attractor lies in the fact that it, together with its attracting surface, defines the boundary between laminar and turbulent. The simple structure with only two vortices suggests that perturbations which set up these vortices should be strongest and most effective in triggering turbulence. So now we have three invariant objects to deal with: an attractor around the laminar profile, the chaotic dynamics in the fully turbulent regime and the chaotic dynamics in the border between laminar and turbulent. The relations and links between them are a matter of ongoing studies and not entirely trivial, as the next observation shows.

Transient turbulent dynamics

The final aspect to be discussed here deals with the issue of the decay of the turbulent state, first emphasized by Brosa [17]. Within the picture that the turbulent dynamics are due to the hopping between the different coherent states, the decay can come about if the trajectory misses one state and relaxes towards laminar. Such transient behaviour is associated with chaotic saddles and typically arises in scattering situations. Theory holds that there is no telling when the turbulent dynamics leave the chaotic saddle, so that there is a constant probability of decay, independent of the time the turbulence was started. This implies that the probability $P(t)$ of remaining turbulent for a time t drops off exponentially [18]. Experiments [19, 20, 21] and direct numerical simulations [22, 23] confirm this expectation. But what happens at higher Reynolds numbers? Surely, the region with turbulence must close off and turn from a chaotic saddle into a persistent attractor? The inverse process, where a closed attractor turns into an open saddle is known as a boundary crisis in the dynamical system literature and involves a global bifurcation [24]. In the absence of any direct evidence for such a bifurcation, we can study the variation of the lifetimes with Reynolds number. As anticipated, the lifetimes increase rapidly with Reynolds number. However, the approach may not be fast enough to give a divergence. Experiments and some numerical simulations [19, 20, 23] point to a divergence in the Reynolds number range 1695 to 1870. Other experiments [21] that cover a wider range of lifetimes give characteristic times that are compatible with an increase that is exponential in Reynolds number.

While the difference between a rapid increase and an actual divergence may not seem of much practical relevance, as both easily give lifetimes beyond experimental reach, it is of significance for the representation of the flow and for issues of control. The presence of dynamical links between turbulent and laminar flows implies that the turbulence can decay at any time; even if it does not decay, the turbulent flow can undergo excursions that come arbitrarily

close to the laminar profile, and hence give rise to huge fluctuations in flow speed or pressure drop. From the control point of view the presence of these links invites speculation that it could be possible to target the flow to return to laminar with minimal effort.

Concluding remarks

The history of pipe flow shows that every aspect understood is countered by new riddles to be resolved. While I do believe that with the ideas outlined above we now have at hand a frame into which we can fit the pieces of the puzzle, many details remain to be resolved, and they surely will provide new surprises. None of this would have been possible without innovative experiments and extensive numerical simulations at the edge of today's computer powers, and further experiments and simulations are welcome. The reward will be a complete theory that not only encompasses pipe flow and other internal shear flows, but hopefully sheds light on bypass transitions in external shear flows as well.

Acknowledgements

I would like to thank Armin Schmiegel, Holger Faisst, and Tobias M Schneider for their admirable dedication and unflinching efforts to uncovering many aspects of this transition; Jeff Moehlis and Jürgen Vollmer for their valuable assistance on dynamical systems matters; Bjorn Hof, Jerry Westerweel and the late Frans T M Nieuwstadt for fruitful collaborations; Tom Mullin and Rich Kerswell for sharing their works before publication; Siegfried Grossmann for constant inspiration; and last but not least the Deutsche Forschungsgemeinschaft for supporting this work.

References

- [1] O.E.Lanford, *Annu Rev Fluid Mech*, **14** (1982) 347
- [2] J.Guckenheimer, *Annu Rev Fluid Mech*, **18** (1986) 15
- [3] P.Holmes, J.L.Lumley and G.Berkooz, *Turbulence, coherent structures, dynamical systems*, Cambridge University Press, Cambridge 1986
- [4] L.Boberg and U.Brosa, *Z Naturforsch* **43a** (1988) 679
- [5] L.N.Trefethen et al, *Science* **261** (1993) 578
- [6] S.Grossmann, *Rev. Mod. Phys.* **72** (2000) 603
- [7] F.Waleffe, *Phys. Fluids* **9** (1997) 883
- [8] B.Eckhardt et al, *Annu Rev Fluid Mech*, **39** (2007)
- [9] H.Faisst and B.Eckhardt, *Phys. Rev. Lett.* **91** (1993) 224502

- [10] H.Wedin and R.R.Kerswell, *J. Fluid Mech.* **508** (2004) 333
- [11] G. Ott and B.Eckhardt, *Z Phys. B* **94** (1994) 259
- [12] B.Hof, C.W.H.van Doorne et al, *Science* **305** (2004) 1594
- [13] T.M.Schneider, J.Vollmer and B.Eckhardt, *Phys. Rev. E* (2007), in press.
- [14] J.Moehlis, H.Faisst and B.Eckhardt, *New J. Phys.* **6** (2004) 56
- [15] J. Skufca, B.Eckhardt, J.A.Yorke, *Phys. Rev. Lett.* **96** (2006) 174101
- [16] T.M.Schneider, B.Eckhardt, J.A.Yorke, *Phys. Rev. Lett.* (2007) submitted.
- [17] U.Brosa, *J. Stat. Phys.* **55** (1989) 1303
- [18] H.Kantz and P.Grassberger, *Physica D* **17** (1985) 75
- [19] J.Peixinho and T.Mullin, *Phys. Rev. Lett.* **96** (2006) 094501
- [20] T.Mullin and J.Peixinho, *J. Low Temp. Phys.* **145** (2006) 75
- [21] B.Hof et al, *Nature* **443** (2006) 59
- [22] H.Faisst and B.Eckhardt, *J Fluid Mech.* **504** (2004) 343
- [23] A.P.Willis and R.R.Kerswell, *Phys. Rev. Lett.* **98** (2007) 014501
- [24] C.Grebogi et al, *Phys. Rev. Lett.* **48** (1982) 1507

EUROMECH Fellows: Nomination Procedure

The EUROMECH Council was pleased to announce the introduction of the category of **EUROMECH Fellow**, starting in 2005. The status of Fellow is awarded to members who have contributed significantly to the advancement of mechanics and related fields. This may be through their original research and publications, or their innovative contributions in the application of mechanics and technological developments, or through distinguished contribution to the discipline in other ways.

Election to the status of Fellow of EUROMECH will take place in the year of the appropriate EUROMECH Conference, EFMC or ESMC respectively. The number of fellows is limited in total (fluids and solids together) to no more than one-half of one percent of the then current membership of the Society.

Nomination conditions:

- The nomination is made by **two sponsors** who must be members of the Society;
- Successful nominees must be members of the Society;
- Each nomination packet must contain a completed Nomination Form, signed by the two sponsors, and no more than four supporting letters (including the two from the sponsors).

Nomination Process:

- The nomination packet (nomination form and supporting letters) must be submitted before 15 January in the year of election to Fellow (the year of the respective EFMC or ESMC);
- Nominations will be reviewed before the end of February by the EUROMECH Fellow Committee;
- Final approval will be given by the EUROMECH Council during its meeting in the year of election to Fellow;
- Notification of newly elected Fellows will be made in May following the Council meeting;
- The Fellow award ceremony will take place during the EFMC or ESMC as appropriate.

Required documents and how to submit nominations:

Nomination packets need to be sent before the deadline of 15 January in the year of the respective EFMC or ESMC to the President of the Society. Information can be obtained from the EUROMECH web page www.euromech.org and the Newsletter. Nomination Forms can also be obtained from the web page or can be requested from the Secretary-General.

NOMINATION FORM FOR FELLOW

NAME OF NOMINEE:.....

OFFICE ADDRESS:.....

.....

.....

EMAIL ADDRESS:.....

FIELD OF RESEARCH:

Fluids: Solids:

NAME OF SPONSOR 1:

OFFICE ADDRESS:.....

.....

.....

EMAIL ADDRESS:.....

SIGNATURE & DATE:

NAME OF SPONSOR 2:

OFFICE ADDRESS:.....

.....

.....

EMAIL ADDRESS:.....

SIGNATURE & DATE:

SUPPORTING DATA

- Suggested Citation to appear on the Fellowship Certificate (30 words maximum);
- Supporting Paragraph enlarging on the Citation, indicating the Originality and Significance of the Contributions cited (limit 250 words);
- Nominee's most Significant Principal Publications (list at most 8);
- NOMINEE'S OTHER CONTRIBUTIONS (invited talks, patents, professional service, teaching etc. List at most 10);
- NOMINEE'S ACADEMIC BACKGROUND (University Degrees, year awarded, major field);
- NOMINEE'S EMPLOYMENT BACKGROUND (position held, employed by, duties, dates).

SPONSORS DATA

Each sponsor (there are two sponsors) should sign the nomination form, attach a letter of recommendation and provide the following information:

- Sponsor's name;
- Professional address;
- Email address;
- Sponsor's signature/date.

ADDITIONAL INFORMATION

Supporting letters (no more than four including the two of the sponsors).

TRANSMISSION

Send the whole nomination packet to:

Professor Patrick Huerre
President EUROMECH
Laboratoire d'Hydrodynamique, École Polytechnique
91128 Palaiseau Cedex, France
E-mail: huerre@ladhyx.polytechnique.fr

EUROMECH- European Mechanics Society: Fellow Application

EUROMECH Prizes: Nomination Procedure

Fluid Mechanics Prize

Solid Mechanics prize

Regulations and Call for Nominations

The *Fluid Mechanics Prize* and the *Solid Mechanics Prize* of EUROMECH, the European Mechanics Society, shall be awarded on the occasions of Fluid and Solid conferences for outstanding and fundamental research accomplishments in Mechanics.

Each prize consists of 5000 Euros. The recipient is invited to give a Prize Lecture at one of the European Fluid or Solid Mechanics Conferences.

Nomination Guidelines:

A nomination may be submitted by any member of the Mechanics community. Eligible candidates should have undertaken a significant proportion of their scientific career in Europe. Self-nominations cannot be accepted.

The nomination documents should include the following items:

- A presentation letter summarizing the contributions and achievements of the nominee in support of his/her nomination for the Prize;
- A curriculum vitae of the nominee,
- A list of the nominee's publications,
- At least two letters of recommendation.

Five copies of the complete nomination package should be sent to the Chair of the appropriate Prize Committee, as announced in the EUROMECH Newsletter and on the Society's Web site www.euromech.org Nominations will remain active for two selection campaigns.

Prize committees

For each prize, a Prize Committee, with a Chair and four additional members shall be appointed by the EUROMECH Council for a period of three years. The Chair and the four additional members may be re-appointed once. The committee shall select a recipient from the nominations. The final decision is made by the EUROMECH Council.

Fluid Mechanics Prize

The nomination deadline for the Fluid Mechanics prize is **15 January in the year of the Fluid Mechanics Conference**. The members of the *Fluid Mechanics Prize and Fellowship Committee* are:

- A. Kluwick (Chair)
- O. E. Jensen
- D. Lohse
- W.Schröder
- Y. Couder

Chairman's address

Professor A. Kluwick
Institut für Strömungsmechanik und Wärmeübertragung
Technische Universität Wien
Resselgasse 3,
A -1040 Wien, Austria
Tel. : +43 1 58801 32220
Fax : +43 1 58801 32299
Email: akluwick@mail.tuwien.ac.at

Solid Mechanics Prize

The nomination deadline for the Solid Mechanics prize is **15 January in the year of the Solid Mechanics Conference**. The members of the *Solid Mechanics Prize and Fellowship Committee* are:

- W.Schiehlen (Chair)
- H. Myhre Jensen
- N.F. Morozov
- M. Raous
- B. A. Schrefler

Chairman's address

Professor W.Schiehlen
Institut für Technische und Numerische Mechanik
Universität Stuttgart
Pfaffenwaldring 9
D-70550 Stuttgart, Germany
Tel. : +49 711 685-66391
Fax : +49 711 685-66400
Email: schiehlen@itm.uni-stuttgart.de

EUROMECH Conferences in 2007, 2008, 2009

The general purpose of EUROMECH conferences is to provide opportunities for scientists and engineers from all over Europe to meet and to discuss current research. Europe is a very compact region, well provided with conference facilities, and this makes it feasible to hold inexpensive meetings.

The fact that the EUROMECH Conferences are organized by Europeans primarily for the benefit of Europeans should be kept in mind. Qualified scientists from any country are of course welcome as participants, but the need to improve communications within Europe is relevant to the scientific programme and to the choice of leading speakers.

A EUROMECH Conference on a broad subject, such as the ESMC or the EFMC, is not a gathering of specialists all having the same research interests, and much of the communication which takes place is necessarily more in the nature of the imparting of information than the exchange of the latest ideas. A participant should leave a Conference knowing more and understanding more than on arrival, and much of that gain may not be directly related to the scientist's current research. It is very important therefore that the speakers at a Conference should have the ability to explain ideas in a clear and interesting manner, and should select and prepare their material with this expository purpose in mind.

2007

EMMC10

10th EUROMECH-MÉCAMAT Conference

DATES: 11-14 June 2007

LOCATION: Kazimierz Dolny, Poland

CONTACT Prof. W.K.Nowacki, IPPT-Polish Academy of Sciences

E-MAIL: wnowacki@ippt.gov.pl

WEBSITE: <http://www.lmt.ens-cachan.fr/emmc10/index.html>

EETC11

11th EUROMECH European Turbulence Conference

DATES: 25 – 28 June 2007

LOCATION: Faculty of Engineering of the University of Porto
Porto, Portugal

CONTACT: Prof. J. M. L. M. Palma, University of Porto

E-MAIL: etc11@fe.up.pt

2008

EMMC11

11th EUROMECH-MÉCAMAT Conference

DATES: 10 – 14 March 2008

LOCATION: Turin, Italy

CONTACT: Prof. J.F. Ganghoffer, Prof. F. Pastrone

E-MAIL: jfgangho@hotmail.com, pastrone@dm.unito.it

ENOC6

6th EUROMECH Nonlinear Oscillations Conference

DATES: 30 June–4 July 2008

LOCATION: St. Petersburg, Russia

CONTACT: Prof. Alexander L. Fradkov ,

E-MAIL: fradkov@mail.ru

EFMC7

7th EUROMECH Fluid Mechanics Conference

DATES: 14 – 18 September 2008

LOCATION: Manchester, UK

CONTACT: Prof. Peter Duck,

E-MAIL: duck@ma.man.ac.uk

2009

EETC12

12th EUROMECH European Turbulence Conference

DATES: 7 – 10 September 2009

LOCATION: Marburg, Germany

CONTACT: Prof. Bruno Eckhardt

E-MAIL: bruno.eckhardt@Physik.Uni-Marburg.de

ESMC7

7th European Solid Mechanics Conference

DATES: August 2009

LOCATION: Lisbon, Portugal

CONTACT: Prof. Jorge Ambrosio

E-MAIL: jorge@dem.ist.utl.pt

EUROMECH Colloquia in 2007 and 2008

EUROMECH Colloquia are informal meetings on specialized research topics. Participation is restricted to a small number of research workers actively engaged in the field of each Colloquium. The organization of each Colloquium, including the selection of participants for invitation, is entrusted to a Chairman. Proceedings are not normally published. Those who are interested in taking part in a Colloquium should write to the appropriate Chairman. Number, Title, Chairperson or Co-chairperson, Dates and Location for each Colloquium in 2007, and preliminary information for some Colloquia in 2008, are given below.

EUROMECH Colloquia in 2007

481. Recent Advances in the Theory and Applications of Surface and Edge Waves

Chairperson: Prof. Yibin Fu

Department of Mathematics, Keele University

Staffordshire ST5 5BG, UK

Phone: +44(0)1782 583650; Fax: +44(0)1782 584268

Email: y.fu@keele.ac.uk

Co-Chairperson: Prof. Julius Kaplunov

Date and location: 11-14 June 2007, Keele University, UK

Website: <http://www.keele.ac.uk/depts/ma/euromech/>

482. Efficient Methods for Robust Design and Optimization

Chairperson: Dr.-Ing. habil. Fabian Duddeck

Department of Engineering

London University, Queen Mary College

Mile End Road, London E1 4NS, UK

Phone: +44(0)20 7882 3749; Fax: +44(0)20 8983 1007,

E-Mail: f.duddeck@qmul.ac.uk

Co-Chairpersons:

Prof. Dr.-Ing. Kai-Uwe Bletzinger,

Prof. Dr. techn. Christian Bucher,

Prof. Hermann G. Matthies Ph.D,

Dr. Marcus Meyer,

Date and location 10-12 September 2007, London, UK

483. Non-linear Vibrations of Structures

Chairperson: Prof. P.L. Ribeiro,

IDMEC/DEMEGI, Faculdade de Engenharia

Universidade do Porto,
Rua Doutor Roberto Frias,
4200-465 Porto, Portugal
Phone: +351 22 508 1713; Fax: +351 22 508 1445
E-mail: pmleal@fe.up.pt
Co-chairperson: Prof. Marco Amabili
Date and location: 9-11 July 2007, University of Porto, Portugal
Website: <http://www.fe.up.pt/nlvs2007>

488. The Influence of Fluid Dynamics on the Behaviour and Distribution of Plankton

Chairperson: Dr. David Lewis
Department of Mathematical Sciences
University of Liverpool
Mathematical Sciences Building
Liverpool, L69 7ZL, UK
Phone: +44(0)151 794 4014; Fax: +44(0)151 794 4061
E-mail: d.m.lewis@liv.ac.uk
Co-Chairperson: Dr. Rachel Bearon
Date and location: 13-15 June 2007, Liverpool, UK
Website: <http://www.liv.ac.uk/math/Euromech488/index.html>

489. Porous Media: Modelling of Multiphase Materials

Chairperson: Prof. Ragnar Larsson
Dept of Applied Mechanics/ Div. of Material and Computational Mechanics
Chalmers University of Technology
S-412 96 Gothenburg, Sweden
Phone: +46 31 7725267; Fax: +46 31 7723827
Email: ragnar@chalmers.se
Co-Chairperson: Prof. Dr.-Ing. Stefan Diebels
Date and location: 19-21 September 2007, Chalmers University of Technology, Gothenburg, Sweden
Website: http://www.am.chalmers.se/~ragnar/Euromech_489_home/

490. Dynamics and Stability of Thin Liquid Films and Slender Jets

Chairperson: Dr. Omar K. Matar
Department of Chemical Engineering
Imperial College London
South Kensington Campus
London SW7 2AZ, UK
Phone: +44(0)207 594 5571; Fax: +44(0)207 594 5629
E-mail: o.matar@imperial.ac.uk
Co-Chairpersons:

Dr. Richard V. Craster
Dr. Andreas Münch
Dr. Thomas P. Witelski

Date and location: 26-28 September 2007, Imperial College, London, UK

491. Vortex Dynamics from Quantum to Geophysical Scales

Chairperson: Dr. Andrew D. Gilbert,
Mathematics Research Institute,
School of Engineering, Computer Science and Mathematics,
University of Exeter,
Exeter EX4 4QE, U.K.

Phone: +44(0)1392 263981; Fax: +44(0)1392 263997

Email: A.D.Gilbert@exeter.ac.uk

Co-Chairpersons:

Dr. Konrad Bajer

Prof. Carlo F. Barenghi

Date and location: 11-14 September 2007, Exeter, U.K

Website: www.secam.ex.ac.uk/~adg/euromech491.html

492. Shear-Banding Phenomena in Entangled Systems

Chairperson: Dr H. J. Wilson

Department of Mathematics

University College London

Gower Street, London WC1E 6BT, U.K.

Phone: +44(0)20 7679 1302; Fax: +44(0)20 7383 5519

Email: helen.wilson@ucl.ac.uk

Co-chairperson: Dr. M. P. Lettinga

Date and location: 3-5 September 2007, London, UK

Website: <http://www.ucl.ac.uk/euromech492/>

493. Interface Dynamics, Stability and Fragmentation

Chairperson: Prof. Emmanuel Villiermaux,

Université de Provence, IRPHE,

49, rue Frédéric-Joliot Curie

13384 Marseille Cedex, France

Phone: +33 4 96 13 97 42 ; Fax: +33 4 96 13 97 09

E-mail: villerma@irphe.univ-mrs.fr

Co-chairperson: Prof. J.Hinch

Date and location: 29-31 August 2007, Grenoble, France

494. Symposium on Micro PIV and Applications in Microsystems

Chairperson: Dr Ralph Lindken

Laboratory for Aero- and Hydromechanics

J. M. Burgers Centrum

Leeghwaterstraat 21
2628CA Delft, The Netherlands
Phone: +31 15 278 2991 ; Fax: +31 15 278 2947
E-mail: r.lindken@wbmt.tudelft.nl
Co-chairperson: Prof. J. Westerweel
Date and location: May 2007, Delft, The Netherlands

EUROMECH Colloquia in 2008

495. Advances in Simulation of Multibody System Dynamics

Chairperson: Prof. Dmitry Pogorelov
Department of Applied Mechanics
Bryansk State Technical University
b.50 let Oktyabrya, 7
241035 Bryansk, Russia
Phone: +7 4832 568637; Fax: +7 4832 568637
Email: pogorelov@tu-bryansk.ru
Co-Chairperson: Em. Prof. Dr.-Ing. Werner Schiehlen
Date and location: 18-21 February 2008, Bryansk, Russia

496. Control of Fluid Flow

Chairperson: Prof. Peter Schmid
Laboratoire d'Hydrodynamique (LadHyX)
Ecole Polytechnique
F-91128 Palaiseau, France
Phone: +33 1 69 333780; Fax: +33 1 69 333030
e-mail: peter.schmid@ladhyx.polytechnique.fr
Co-Chairperson: Dan Henningson
Date and location: May 2008, Paris, France

497. Recent Developments and New Directions in Thin-Film Flow

Chairperson: Prof. Stephen K. Wilson
Department of Mathematics
University of Strathclyde,
Livingstone Tower
26 Richmond Street
Glasgow, G1 1XH, UK
Phone: +44(0)141 548 3820; Fax: +44(0)141 548 3345
E-Mail: s.k.wilson@strath.ac.uk
Co-Chairperson: Dr. Brian R. Duffy,
Date and location: Summer 2008, Edinburgh, UK

498. Nonlinear Dynamics of Composites and Smart Structures

Chairperson: Prof. J. Warminski
Lublin University of Technology
Department of Applied Mechanics
Nadbystrzycka 3620-618, Poland
Ph: +48 81 538 4197; Fax: +48 81 538 4205
E-mail: j.warminski@pollub.pl
Co-Chairperson: Dr. M.P.Cartmell
Date and location: 21 – 24 May 2008, Kazimierz Dolny, Poland

499. Nonlinear Mechanics of Multiphase Flow in Porous Media: Phase Transitions, Instability, Non Equilibrium, Modeling

Chairperson: Mikhail Panfilov
LEMTA-ENSEM
2, av. de la Foret de la Haye
BP 160
F-54504 Vandoeuvre-les-Nancy Cedex, France
Ph: +33 3 83595697, Fax: +33 3 83595616
E-mail: mikhail.panfilov@ensem.inpl-nancy.fr
Date and location: May-June 2008, Institut National Polytechnique de Lorraine, Nancy, France

500. Non-smooth Problems in Vehicle Systems Dynamics - Analysis and Solutions

Chairperson: Prof. Per Grove Thomsen
Technical University of Denmark
Richard Petersens Plads 321
DK-2800 Kgs. Lyngby, Denmark
Ph: + 45 45253073, Fax : +45 45932373
E-mail: pgt@imm.dtu.dk
Co-Chairperson: Prof. Hans True
Date and location: 17 - 20 June 2008, Danish Technical University, Lyngby, Denmark

501. Mixing of Coastal, Estuarine and Riverine Shallow Flows

Chairperson: Prof. Maurizio Brocchini
Istituto di Idraulica e Infrastrutture Viarie,
Università Politecnica delle Marche,
60131 Ancona, Italy
Ph: +39 071 220 4522, Fax: +39 071 220 4528
E-mail: m.brocchini@univpm.it
Co-Chairperson: Prof. GertJan van Heijst
Date and location: 8 - 11 June 2008, Istituto di Idraulica e Infrastrutture Viarie, Ancona, Italy

502. Reinforced Elastomers: Fracture Mechanics Statistical Physics and Numerical Simulation

Chairperson: Prof. G. Heinrich

Leibniz Institut für Polymerforschung Dresden e. V.

Postfach 120411

01005 Dresden, Germany

Ph: +49 0 351 4658 360, Fax: +49 0 351 4658 362

E-mail: gheinrich@ipfdd.de

Co-Chairperson: Prof. Erwan Verron

Date and location: October 2008, Leibniz Institut für Polymerforschung Dresden e.V., Germany

EUROMECH Colloquia Reports

EUROMECH Colloquium 475

"Fluid Dynamics in High Magnetic Fields"

1 - 3 March 2006, Technische Universität Ilmenau, Germany

Chairpersons: Thierry Alboussiere (LGIT Grenoble), Sergej Molokov (Coventry University), Alban Pothérat (TU Ilmenau), André Thess (TU Ilmenau)

Flows of electrically conducting fluids like mercury, seawater, liquid steel, semiconductor melts, and molten glass can be controlled by electromagnetic (Lorentz) forces in a variety of ways. Traditionally, fundamental and industrial fluid dynamics research in this field has been focused on the effects of "ordinary" magnetic fields, produced by traditional electromagnet providing around one Tesla. This colloquium was focused on phenomena in fields of 5 to 15 Tesla. These so-called "high" magnetic fields are now becoming accessible to the fluid dynamics community thanks to the increasing availability of warm bore cryofree superconducting magnets. In particular, these magnets make it possible to investigate magnetohydrodynamic (MHD) turbulence in transparent fluids like electrolytes, in which powerful optical measurement techniques such as Laser Doppler Anemometry or Particle Image Velocimetry can be used, unlike in liquid metals.

This colloquium gathered researchers from different communities including MHD, flow measurement, material processing, applied maths and nonlinear physics around the idea of using high magnetic fields for the control of fluid flows in electrically conducting, para- or diamagnetic fluids. Researchers from the fluid dynamics community were encouraged to take advantage of the infrastructure of the Grenoble High Magnetic Field Laboratory. Also the participants were invited to make use of the available 5-Tesla superconducting magnet at Ilmenau University.

The colloquium was opened on 1 March 2006 with an invited lecture by Dr. Francois Debray who presented the technical capabilities of the Grenoble High Magnetic Field Laboratory and invited the participants to use this unique infrastructure. The invited lecture was followed by contributed lectures from B. Hamann and S. Molokov and by a laboratory visit to the MHD facilities of TU Ilmenau.

During the second day two invited lectures were given, one by Professor Alfred Leder of Rostock University and another by Professor Hideyuki Yasuda. Professor Leder provided a comprehensive overview of the methods of optical flow measurement. These methods could be used for MHD-experiments in transparent fluids in combination with a high magnetic field. Professor Yasuda demonstrated how a strong magnetic field can affect solidification. The speaking time of 30 minutes (including discussion) gave participants ample opportunity for discussion and questions.

The last day was devoted to turbulent MHD flows including those of a geophysical nature and for non-zero magnetic Reynolds number. The theoretical contributions raised many questions that might be answered in future experiments in high magnetic fields.

During the final discussion many participants expressed the view that this was a very successful meeting and that they were interested in meeting again in the future. We thank EOREMECH for supporting the meeting and for making it possible.

Two broad approaches exist to deal with the simulation of deformable interfaces in multiphase flows: (i) deformable grids, adapted locally to the interface, and (ii) fixed grids, with a separate procedure to describe the position of the interface. There are several fixed-grid methods, which differ mostly in the way they deal with the interface. They include classical front-tracking, volume-of-fluid, level-set, and boundary integral methods. Usually they can be classified into front-tracking and front-capturing, depending on whether the position of the interface is followed or captured within the fixed grid. Fixed-grid methods are very versatile, and they have been used increasingly to simulate complex multiphase flows. At the same time, new variants and improvements of the methods are frequently published, often combining characteristics of several methods and defying standard classifications. These different methods are often used to simulate similar problems, with sometimes conflicting claims on their advantages/disadvantages.

The goal of the colloquium was to bring together the developers and users of the numerical techniques to solve real complex problems, such as the behaviour of buoyant drops/bubbles and the break-up of a liquid jet. The focus was on fixed-grid techniques. The scientific program consisted of three invited lectures: by Dr. Herrmann (Stanford), focusing on level-set techniques; by Prof. G. Tryggvason (Worcester) focusing on front tracking techniques; and by Prof. Zaleski (Paris), focusing on volume-of-fluid techniques. In addition to the invited lectures, 29 presentations were given on front-tracking, volume-of-fluid, level-set methods, or a combination of them. The presentations gave a good overview of the state of the art of the field, regarding the numerical techniques and their applications. From the technique-development perspective, it became clear that there is a need for physically based (sub-grid) models for coalescence and break-up. Some impressive recent results were presented, showing the potential for different techniques to tackle real complex problems. Overall, the quality of both the presentations and the discussions was quite high, and the participants were enthusiastic about a very successful colloquium.

EUROMECH Colloquium 480

“High Rayleigh Number Convection”

4–8 September, 2006, Trieste, International Centre for Theoretical Physics

Chairperson: Prof. Detlef Lohse, Twente

Co – chairperson: Prof. Roberto Verzicco, Bari

Colloquium 480 was held at the International Centre for Theoretical Physics (ICTP) in Trieste, Italy. Its objective was to discuss physical phenomena and recent developments in the field of thermally driven turbulence which involves countless aspects of natural and technological problems.

There were about 50 participants from 20 different countries and about 40 presentations. These included eight key-note lectures by: K.Q. Xia (Hong Kong), A. Thess (Ilmenau), M. Sano, (Tokyo), P. Roche (Grenoble), J. Niemela (Trieste), F. Busse (Bayreuth), and an evening Public Lecture by L. Kadanofi (Chicago). The Colloquium also hosted a special session in honour of the 70th birthday of Prof. F. Busse. The quality of the presentations was very high and the following discussions were very active. In several cases the discussion had to be interrupted in order to keep the schedule. Special discussion sessions were organized after the talks and in addition there was time for informal discussions between the participants. A notably high proportion of the participants attended all the talks.

The main topics addressed in the talks and the discussions were:

- **Heat flux at $Ra > 1011$:**

The discrepancy between heat transfer measurements in two apparently identical cryogenic experiments for the Nusselt number beyond $Ra > 1011$ cannot yet be resolved. Many different possibilities were investigated, such as sidewall imperfections, and plate extensions, but none of them could explain the differences.

- **Non Oberbeck Boussinesq effects**

In many experimental investigations, high Rayleigh numbers are obtained by going to larger temperature differences than allowed within the Boussinesq approximation. Several papers have discussed in detail the non-Oberbeck Boussinesq effects on the flow, when the temperature dependence of the fluid properties is non negligible. The different behaviour of liquids and gasses has shown that the $\alpha\Delta$ product, where α is the thermal expansion coefficient and Δ the total temperature difference, might not be adequate to fully characterize the Boussinesq regime.

- **Spatial distribution of the thermal dissipation rate**

Following the unifying model of thermal convection, based on a decomposition of the kinetic and thermal energy dissipations, the spatial distribution of the thermal dissipation rate has been investigated by numerical simulations and experiments. Although many interesting observations have been made, the difficulty in characterising the thermal plumes in a strongly turbulent environment still limits the analysis and further investigation is required.

- **Mean wind dynamics**

The large scale recirculation in a Rayleigh Benard cell has been observed to experience sudden reorientations and reversals whose statistics were studied in detail. It has been pointed out that even minor imperfections or misalignments in the experimental set up can produce drastic changes in the flow statistics, thus explaining major differences in apparently similar experiments.

- **Flow with background rotation**

When the system is put in rotation, an additional forcing comes into play and the flow dynamics change. In particular the combined effects of the Taylor Proudman theorem and of Ekman pumping can increase or inhibit the heat transfer depending on the particular flow parameters.

Many key questions are still far from being answered and further investigation is needed. The community resolved to meet again in Lyon during 2009. We thank the International Centre for Theoretical Physics and EUROMECH for making the Meeting possible, and for all the financial and organizational support.

EUROMECH Colloquium 484

“Wave Mechanics and Stability of Long Flexible Structures Subject to Moving Loads and Flows”

19–22 September, 2006, TU Delft, The Netherlands

Chairperson: *Andrei V. Metrikine, Delft, The Netherlands*

Co – chairpersons: *L. Frýba, Czech Republic; Emmanuel de Langre, France*

A number of modern engineering structures, such as continuously welded railway tracks, deep water offshore risers and long-span suspension bridges, are so long that the dynamic processes in their interior are hardly influenced by the boundaries. To predict the dynamic behaviour of these structures correctly, it is necessary to consider them as infinitely long waveguides and to model their behaviour using the theory of wave processes.

The aim of EUROMECH Colloquium 484 was to discuss the methods of analytical, numerical and experimental analysis of long flexible structures subjected to moving loads and flows. The focus of the discussion was on the flow-induced and moving-load-induced wave processes and dynamic instabilities as these phenomena are of major importance in Civil, Mechanical and Offshore Engineering.

There were altogether 54 participants from 16 countries and 49 presentations, including two key-note lectures by Michael Paidoussis (Montreal, Canada) and Iliya Blekhman (St. Petersburg, Russia). A number of well-known researchers attended the Colloquium, including the Editor-in-Chief of the Journal of Fluids and Structures and 2 Associate European Editors of the Journal of Sound and Vibration. The Colloquium was opened by the Rector of TU Delft, Professor Jacob Fokkema. All lectures, coffee breaks, and lunches were organized in one building which facilitated a non-stop exchange of ideas both in the lecture rooms and at the coffee-corners.

The Colloquium sessions were organized such that there were daily sessions devoted to (i) flow-induced vibrations and waves; (ii) dynamic processes induced by moving loads; (iii) general theory of wave processes in mechanical systems. This type of organization helped to unify the specialists in ‘wet’ physics of fluid-structure interaction and ‘dry’ physics of moving-load-structure interaction. The presence of a number of specialists in the general theory of vibrations and waves was highly beneficial.

The following challenging problems were discussed during the Colloquium:

- **Vortex Induced Vibration (VIV) of long pipes in water currents**

No reliable procedure to predict vibration of long submerged pipes in currents appears to exist. The term 'long' implies here that more than one mode of the pipe can synchronize with the vortex field around the pipe. The available Fluid Dynamic Codes are not powerful enough to simulate 3D fluid-structure interaction in the range of practically interesting Reynolds numbers (higher than 10^4). The frequency domain iteration procedures that utilize the frequency-amplitude relationships measured in the forced-vibration tests also fail to predict dynamics of long pipes correctly. Time-domain phenomenological models developed from the wake oscillator model seem to be one of the few promising alternatives.

- **Soil vibration induced by high-speed trains**

The most promising approach to predicting vibration induced by high speed trains combines the Fourier integral transform over time and the axial coordinate with subsequent employment of the coupled boundary-finite element formulation in the frequency-wavenumber domain. This approach is applicable as long as the model is linear and homogeneous along the railway track. An extension is possible to the periodically-inhomogeneous models, provided that instead of the Fourier transform over the axial coordinate the Fouquet theorem or a so-called periodicity condition is applied. Calculation time remains an issue. It seems that simplified models should be more widely used when applicable. The most challenging issue remains implementation of the non-linear soil behaviour. No break-through is in prospect regarding this issue.

- **Destabilization of slender structures by axial flows**

Both internal (pipe flow) and external (wind along a panel) axial flows can destabilize elastic structures. The destabilization can be due either to interaction along the length of the structure or to boundary effects. The latter appear to be not well understood as yet, because the flow around an edge or an end of the structure is normally very complex. For example, an experimental study of a submerged pipe sucking up water showed that no existing theory can explain the experimentally observed unstable behaviour.

Besides the above formulated topics, a wide variety of ideas, applications and methods in the field of wave mechanics were discussed during the Colloquium. These included:

- the idea of dynamic materials, whose properties can be changed by a running-through wave;
- an idea that a moving load, likewise a particle in relativistic mechanics, should be considered to have an effective mass that grows as the load speed approaches the speed of elastic waves in a continuum;
- an idea that a high-frequency wave can be efficiently excited by a low-frequency wave via the phase-group synchronism (note that excitation of high-frequency vibrations of an oil reservoir with the help of a low-

frequency wave sent from the ground surface is a dream of all oil companies);

- an idea as to how to model solitons in highly-dispersive media;
- web-structures in space, including the Earth-Moon elevators;
- conveyer belts with edge imperfections;
- identification of structural parameters from the response to moving loads in application to bridges under high-speed trains;
- a method to distinguish between the local and global instabilities in translating continua;
- a method to predict the propagation velocity of a phase transition zone.

All researchers interested in the papers presented during the Colloquium are invited to visit the Colloquium website www.euromech484.nl, which will be operational until January 2008. A book of the Colloquium abstracts can be downloaded from this website. Selected papers will be published in a special issue of the Journal of Sound and Vibration that is due to appear in 2007. Many participants expressing their gratitude to the Organizing Committee for a well-organized event, which they liked both scientifically and socially.

EUROMECH Colloquium 487

“Structure Sensitive Mechanics of Polymer Materials: Physical and Mechanical Aspects”

10-13 October 2006, Strasbourg, France

Chairperson: Professor Yves REMOND

Co – chairpersons Professor Stanislav PATLAZHAN

EUROMECH Colloquium 487 was organized by the Institute of Mechanics of Fluids and Solids ULP-CNRS (Strasbourg, France) and the Semenov Institute of Chemical Physics of the Russian Academy of Sciences (Moscow, Russia). The meeting aimed to enhance interactions between mechanicians and physicists concerning novel trends in theoretical and experimental investigations of coupling between deformation behavior and structural evolution of polymeric materials. The following topics were discussed in the Colloquium:

- constitutive modeling of structure sensitive deformation processes in semi-crystalline and amorphous polymers;
- experimental and theoretical studies of physical origin of strain-induced structural transitions in solid polymers;
- structure and ultimate properties of polymer materials including nano-composites, rubbers, and foams;
- localization processes (shear banding, crazing) in semi-crystalline, glassy, and cured polymers.

There were 63 communications in all, including 15 plenary lectures, 31 oral communications, and 17 posters. The 45-minute plenary lectures and the 20-minute oral presentations facilitated informal and penetrating discussions about problems of mutual interest. The program included 14 sessions, with 4 on each of the first three days, chaired by leading experts in structural mechanics and physics of polymer materials.

The contributors to the Colloquium presented comprehensive experiments and modeling of the structure sensitive mechanical behavior and mechanically induced structural transitions of various polymeric materials. The physical origin of the considered phenomena was discussed within a framework of molecular, nano-, micro- and macro-scale approaches. Along with the recognized experts and young scientists in mechanics and physics of polymeric materials, 13 PhD students presented their research.

The abstracts of the contributions were collected and published in a Colloquium Book of Abstracts. Papers presented at the Colloquium will be published in *Polymer Science A*.

The discussion at the meeting was intensive and fruitful, reflecting wide interest in problems discussed at the Colloquium.

Objectives of EUROMECH, the European Mechanics Society

The Society is an international, non-governmental, non-profit, scientific organisation, founded in 1993. The objective of the Society is to engage in all activities intended to promote in Europe the development of mechanics as a branch of science and engineering. Mechanics deals with motion, flow and deformation of matter, be it fluid or solid, under the action of applied forces, and with any associated phenomena. The Society is governed by a Council composed of elected and co-opted members.

Activities within the field of mechanics range from fundamental research on the behaviour of fluids and solids to applied research in engineering. The approaches used comprise theoretical, analytical, computational and experimental methods. The Society shall be guided by the tradition of free international scientific co-operation developed in EUROMECH Colloquia.

In particular, the Society will pursue this objective through:

- The organisation of European meetings on subjects within the entire field of mechanics;
- The establishment of links between persons and organisations including industry engaged in scientific work in mechanics and in related sciences;
- The gathering and dissemination of information on all matters related to mechanics;
- The development of standards for education in mechanics and in related sciences throughout Europe.

These activities, which transcend national boundaries, are to complement national activities.

The Society welcomes to membership all those who are interested in the advancement and diffusion of mechanics. It also bestows honorary membership, prizes and awards to recognise scientists who have made exceptionally important and distinguished contributions. Members may take advantage of benefits such as reduced registration fees to our meetings, reduced subscription to the European Journal of Mechanics, information on meetings, job vacancies and other matters in mechanics. Less tangibly but perhaps even more importantly, membership provides an opportunity for professional identification; it also helps to shape the future of our science in Europe and to make mechanics attractive to young people.



EUROPEAN MECHANICS SOCIETY

COLLOQUIA

CONFERENCES

HOME

ABOUT

STRUCTURE

COLLOQUIA

CONFERENCES

PRIZES & AWARDS

FELLOWS

E V E N T S

3 May 2007
Symposium on Micro PIV and Applications in Microsystems

11 June 2007
EMMC10

11 June 2007
Recent Advances in the Theory and application of surface and edge waves

13 June 2007
The Influence of Fluid Dynamics on the Behaviour and Distribution of Plankton

25 June 2007
EETC11

9 July 2007
Geometrically Non-Linear Vibrations of Structures

29 August 2007
Interface Dynamics, stability and Fragmentation

3 September 2007
Shear-banding phenomena in entangled systems

EUROMECH - European Mechanics Society is an international non-governmental non-profit scientific organization.



BECOME A MEMBER!
Annual membership: 24 €
5-year membership: 100 €

Renew your membership!

Join

The **OBJECTIVE** of the Society is to engage in all activities intended to promote in Europe the development of mechanics as a branch of science and engineering. Mechanics deals with motion, flow and deformation of matter, be it fluid or solid, under the action of applied forces, and with any associated phenomena.